



ISSN: 2350-0328

**International Journal of Advanced Research in Science,
Engineering and Technology**

Vol. 3, Issue 8 , August 2016

Sensor-less Speed Control of BLDC Motor using NLMS Filter Algorithm

N.Jayamary Sujatha (M.E.), M.Saravanan (M.E., Ph.D.)

Electronics and Communication Engineering, University College of Engineering, Ramanathapuram-623513, India
Electrical and Electronics Engineering, Thiagarajar College of Engineering, Madurai-625015, Tamilnadu, India

ABSTRACT: In low and medium speed non-sinusoidal brushless motor drives, unbalancing in hall position signals cause high current ripples since all rotor position signals are sensed on a continuous basis, requiring an optical encoder or a resolver or expensive hall-effect sensors. This paper sets forth straightforward and easily implemented simple algorithmic procedure for the speed control of BLDC motor using an normalized least mean square (NLMS) filter. The LMS filter toolbox is taken out from the software package MATLAB/SIMULINK. It is used to obtain the required speed characteristics curve for the specified motor parameters designed for definite mathematical model of BLDC motor. In this control strategy, position signals are sensed automatically for certain speed under any load condition. Normalized least mean square algorithm iterate each tap weight in the direction of gradient of squared magnitude of error between actual speed and reference speed of BLDC motor on specified motor operating condition. Hysteresis current controller provides gate-triggering signals from position signal acquiring by the output of NLMS filter. Ripple less supply currents are produced for six- step operation of BLDC motor. Finally, all characteristics of constant DC voltage BLDC motor are simulated and its characteristics are analysed experimentally for changeable loaded condition without using high cost position sensors. As well, the better, faster performance of NLMS filter is articulated with existing PID controller with all necessary outcomes.

KEYWORDS: Brushless DC Motors, Variable Speed Drives, PWM inverters, Adaptive Filters, Electric Sensing Devices, Filtering Theory, Hall Effect Devices

I. INTRODUCTION

Trapezoidal back EMF permanent magnet direct current [D.C] motors encompass a number of advantages related with brush direct current motors [1]. They have a small maintenance due to the removal of mechanical commutation. Brushless DC motors (BLDC) are frequently employed for many industrial applications owing to their high power efficiency, high torque bears up capability and high motor power density [2]. The permanent magnet brushless DC motors (PMBLDC) can be handled in both sensor technique and sensorless technique. In sensor method, either a hall sensor, optical encoder, resolver or other shaft position sensor is applied to provide the position information for commutation. In the sensorless scheme, fewer modes are not self-starting. During sensor-less operation of BLDC motor, [3] zero crossing detection signals of phase or line back EMFs are essential for exact commutation of motor phase currents. In order to sense the back EMF [4], the motor must be started and brought up to a certain speed value. After the motor speed attains an assured adequate speed, the back EMF of the motor can be identified by the position information with which motor drive switches to synchronous commutation mode. This open-loop start-up can be suitable for a light load, like fan applications. On the other hand, for a few industrial applications, e.g., automotive, fuel pump control, engine control and electric vehicle control, the start-up of the motor has to be made very fast and it is extremely hard to tune the start-up of the motor by means of the open-loop starting algorithm. These applications employ advanced control algorithms in the semi closed loop in which speed control loop does not include the current control loop or in total closed loop, which includes both current control and speed control loop. In this paper [5], the back-EMF voltages are intended using an analogue-to-digital converter. The back-EMF voltage change rate is designed from the measured values and exploited to evaluate the commutation point (CP) by making use of the least-square method. In this paper [6], an adaptive flux observer is introduced with a stator current and flux vector components as state variables and rotor speed is an unknown parameter, which is predictable by using an adaptive scheme. It is an intelligent sensor-less control approach for self-tuning [7]. It precisely adjusts the commutation instant for attaining optimal torque creating capability. A newly proposed method is expressed as the 'equal inductance method' [8] for commutation control. Starting routine is equal to that acquired when using Hall sensors. This study

suggests one rotor position approximation method by sensing the stator currents below every pulse-width modulation of switching position for an interior permanent magnet synchronous motor drive scheme. In this proposed sensorless motor drive [9], the method can be functional in an air conditioner without introducing any high frequency sinusoidal or cosine voltage signal. In this learning [10], the braking commutation approaches investigated as termed with the number of power switches in action over each commutation state. The commutation signals are taken out directly from the average terminal voltages. This proposed method is particularly appropriate for various low power electric vehicles such as electric bicycles, electric scooters, and electric wheelchairs. In brushless DC (BLDC) drives [11-12], power electronic devices existing in an inverter bridge accomplish commutation. Triggering of the power electronic devices has to be made matching with rotor position. Resolving of rotor position, with or without sensor is an important constraint. In general, a common sensorless method is a basis of recognition of the zero crossings of back EMF signals. This mechanism of running is capable for only above a certain speed. BLDC motors exclusively based on back EMF signals for commutation endures from relatively poor starting performance. Always back EMF voltage is referred to the motor neutral point and the zero-crossing of the back EMF is useful for motor commutation. In the majority of all cases, the motor neutral point is not obtainable. As well, a speed estimator circuit is required. Consequently, a special starting algorithm is deliberated to start up the motor from a standstill and accelerate it up to the changeover speed with the feasible rotor position angle. One of the primarily used starting technique is [13]” align then go.” In this technique, the rotor of the BLDC motor aligns to the specific position by energizing any two-phase stator winding and then accelerating the rotor enforced (reference speed) speed according to the commutation sequence. Simulation of sensorless controlled PMBLDC motor is permitted out by trapezoidal using normalized least mean square algorithm for the smooth starting. In addition, the controller can estimate the motor speed and give PWM (Pulse Width Modulation) duty cycle accordingly. The error in the assessment of the rotor position is surrounded by a limit, which is self-governing of operating conditions using NLMS filter. This designed scheme is a fast controller in which simple algorithmic steps and mathematical equations are intended. Tuning of controller’s parameters is not requested for varying reference values of torque, speed. The motor commutation decision can be optimized over the wider speed range of operation. The experimentally replicated results are confirmed with given concept and good performance.

II. BLDC MOTOR MATHEMATICAL MODEL

The BLDC motor mathematical modelling is prepared based on the subsequent assumptions [14-15]:

The three-phase stator winding is symmetrical; the air-gap magnetic field is an ideal square wave. The effect of commutation and armature reaction is ignored. The stator’s surface is asymmetrical; a magnetic circuit is not saturated nevertheless of the eddy current and hysteresis loss. Preferably, air gap fluxes are square wave interaction with rectangular stator current; three phases motor winding synthesis yields trapezoidal back EMF shown in figure.1.2. Permanent magnet brushless DC motor’s air gap flux density waveform should be circulated as square waveforms. According to the motor’s equation of voltage balance, the neutral point node voltage (V_{n0}) of BLDC motor is formed by the subsequent equations:

$$V_{n0} = 1/3 * (V_{a0} + V_{b0} + V_{c0}) - [e_{an} + e_{bn} + e_{cn}] \quad (1)$$

Where, V_{n0} - Neutral point node voltage.

V_{a0} , V_{b0} , V_{c0} - Stator phase voltages.

e_{an} , e_{bn} , e_{cn} - Back EMFs applied in the respective stator phases. Consequently, in this model, allowing for the symmetrical distribution of stator windings, stator resistance per phase is specified by $R_a = R_b = R_c$ and inductance per phase is specified by $L_a = L_b = L_c$. In this paper, unsymmetrical distribution of resistances and inductances is not considered. Always; three phase stator windings are identical design to balance three phase star winding currents and voltages. This is not suitable for NLMS filter sensorless control. Also, NLMS filter sensorless control could not tolerate, when there is a maximum difference in stator winding resistance, inductance, and mutual-inductance. Stator phase voltages with respect to the neutral point are particularly by the following equations (2)-(4) and resulted by means of PMBLDC motor’s inverter circuit (figure.1.1).

$$V_{an} = V_{a0} - V_{n0} \quad (2)$$

$$V_{bn} = V_{b0} - V_{n0} \quad (3)$$

$$V_{cn} = V_{c0} - V_{n0} \quad (4)$$

Where V_{an} , V_{bn} , V_{cn} are stator phase to neutral voltages.

Back EMFs and stator phase voltages are related by equations (5)-(7).

$$V_{an} = i_a R_a + L_a (di_a/dt) + e_{an} \quad (5)$$

$$V_{bn} = i_b R_b + L_b (di_b/dt) + e_{bn} \quad (6)$$

$$V_{cn} = i_c R_c + L_c (di_c/dt) + e_{cn} \quad (7)$$

Where, i_a, i_b, i_c are stator phase currents.

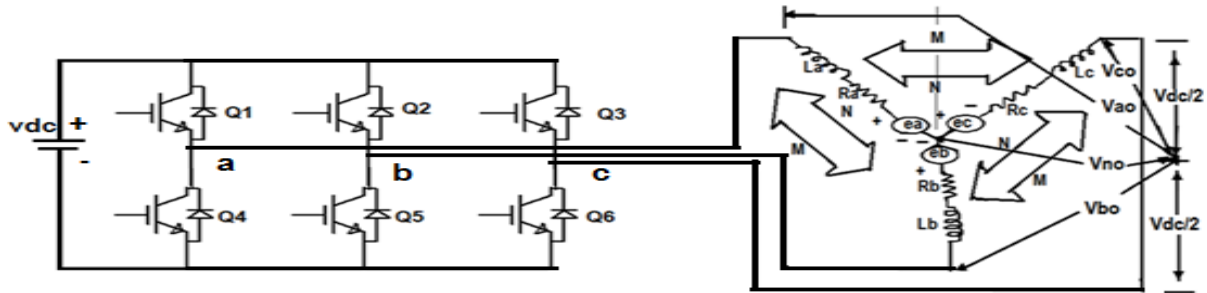


Fig.1. 1 PMBLDC motor's inverter circuit

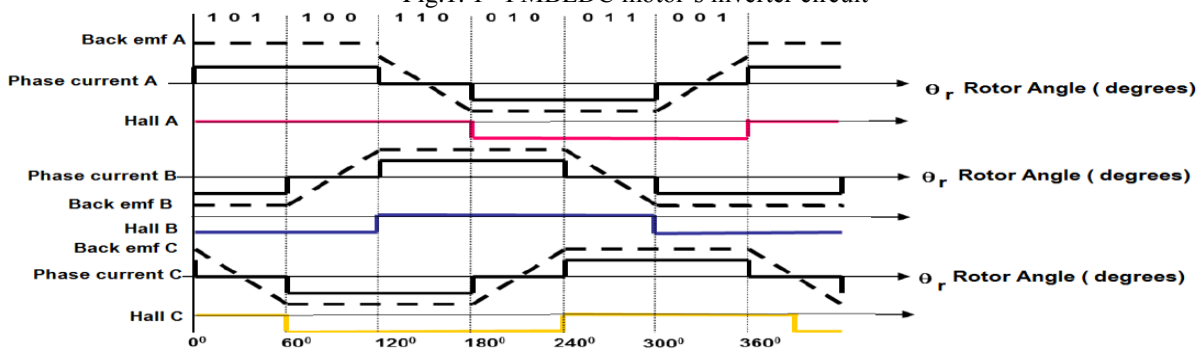


Fig.1. 2 PMBLDC motor's back EMFs and corresponding stator currents

1.2

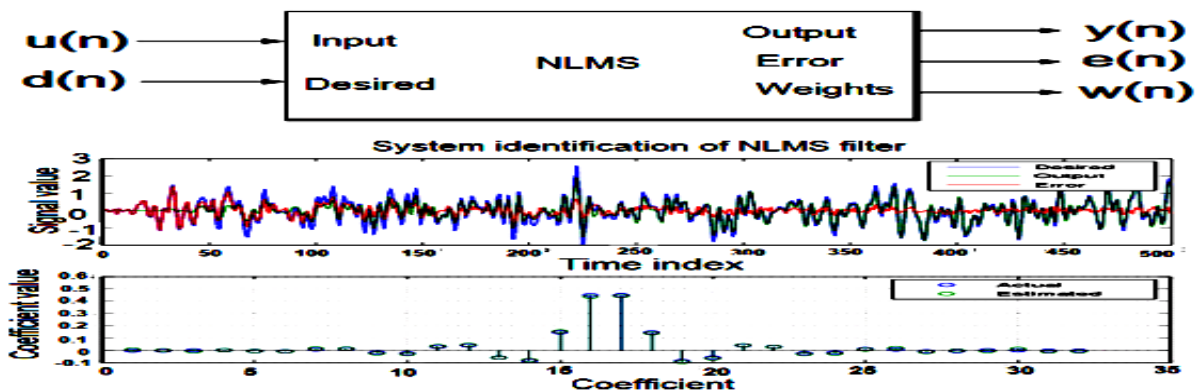


Fig.1. 3 NLMS filter and its performance on signal analysis

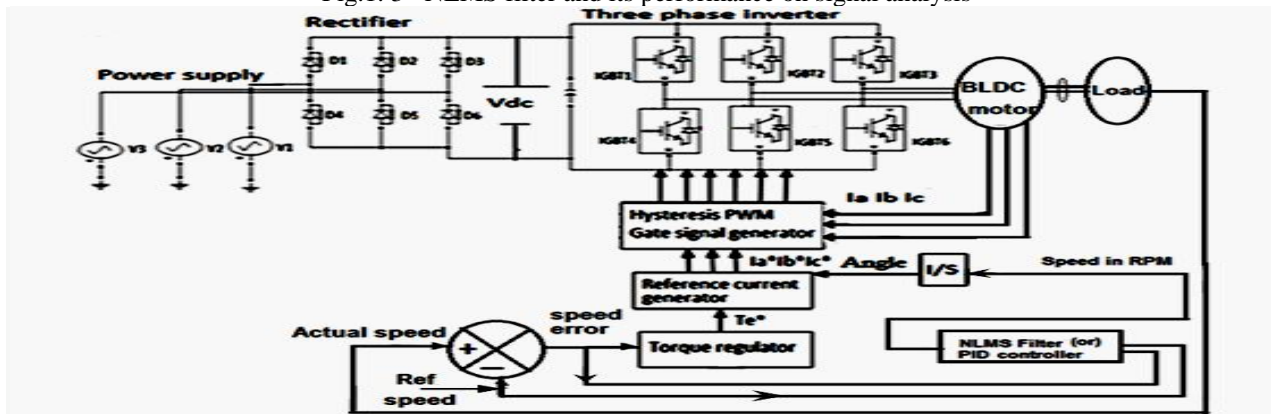


Fig.1. 4 The overall block diagram of developed model of BLDC motor drive

Back EMFs in BLDC motor are calculated using equations (8)-(9).

$$\begin{pmatrix} e_{an} \\ e_{bn} \\ e_{cn} \end{pmatrix} = E \begin{pmatrix} f_a(\theta) \\ f_b(\theta) \\ f_c(\theta) \end{pmatrix} \quad (8)$$

$$E = \omega_r * k_b \quad (9)$$

Where k_b is back-EMF constant, $f_a(\theta)$, $f_b(\theta)$ and $f_c(\theta)$ are the trapezoidal shape function of rotor position, and ω_r is the speed in rad/sec, θ is rotor electrical position.

The stator three-phase currents are estimated as,

$$i_a = [V_{an} - E_{an} - i_a * R_a] * [1/Ls] \quad (10)$$

$$i_b = [V_{bn} - E_{bn} - i_b * R_b] * [1/Ls] \quad (11)$$

$$i_c = [V_{cn} - E_{cn} - i_c * R_c] * [1/Ls] \quad (12)$$

The electromagnetic torque (T_e) of BLDC motor using back-EMFs as follows:

$$T_e = [E_{an} * i_a + E_{bn} * i_b + E_{cn} * i_c] / \omega_r \quad (13)$$

Using dynamic model of motor equation,

$$\omega_m = [(P/2J) * (T_e - T_L - B * \omega_r)] * 1/p \quad (14)$$

Where, T_e is the electromagnetic torque Nw-m, T_L is the load torque in Nw-m, J is the moment of inertia in Nw-sec²/rad, B is the frictional coefficient in Nw-m/ rad/sec, ω_m is rotor speed in mechanical rad/sec, ω_r is rotor speed in electrical rad/sec, P -is the no of poles, “p” is the differential operator (d/dt) and “s”-is the Laplace operator.

The relation between angular speed in mechanical and angular speed in electrical is given by,

$$\omega_m = (P/2) * \omega_r \quad (15)$$

We know the motor speed in electrical,

$$d(\theta)/dt = \omega_r \quad (16)$$

From equation (16) rotor displacement in electrical degrees can be found out as,

$$\theta = (1/s) * \omega_r \quad (17)$$

From (Figure.1.4), BLDC motor drive consists of NLMS filter or PID controller, gate signal generator, IGBT based Inverter, PMBLDC motor, reference current generator, hysteresis PWM gate signal generator, torque regulator. Speed error and reference speed signals are given to NLMS filter [16].

The values of speed error are in the range of positive and negative and the value of reference speed signals are given to NLMS filter. In NLMS filter algorithm, the block calculates the filter weights using the NLMS algorithm equations. Every time the block fills the weights, it replaces the error term with +1 when the error term is positive, -1 when it is negative or 0 when it is zero. It also substitutes every sample of the input vector with +1 when the input sample is positive, -1 when it is negative or 0 when it is zero. The error and the level of noise are restricted by the length of the filter, the number of coefficients or taps. Torque regulator delivers torque reference signal for reference current generator [17].

NLMS filter produces three-phase rotor position signals for essential (reference speed) speed with which motor must run. Motor feedback phase currents are recognized for gate signal generator block to generate gate-triggering pulses by using hysteresis current controller PWM technique.

III. NORMALIZED LEAST MEAN SQUARE (NLMS) ALGORITHM AND ITS IMPLEMENTATION

The Least Mean Square algorithm was greatly first introduced by Widrow and Hoff in 1960[18], is the most widely used adaptive filter algorithm. The Least Mean Square (LMS) algorithm comes under the family of most important stochastic gradient linear adaptive filter algorithm. It is called as a popular stochastic gradient algorithm because it iterates each filter tap weight in the direction of the gradient value of the squared magnitude of the error signal. One of the main disadvantages of the Least Mean Square (LMS) algorithm is having a fixed step-size for the each iteration. One way to overcome this limitation is to use the Normalized Least Mean Square (NLMS) algorithm.

The Normalized Least Mean Square (NLMS) algorithm is very simple [19], but the most robust variant of the Least Mean Square (LMS) algorithm. To analyse the convergence of the adaptive filters NLMS and LMS, the mean-square error (MSE), the minimum mean-square error (MMSE) and the excess mean-square error (EMSE) are computed. NLMS filter gives better performance than LMS filter with small values of MSE, MMSE, and EMSE. It provides a better balance between simplicity and performance than the other types of LMS algorithm and has been given as most

important algorithm in real time applications. Furthermore, it provides many advantages over the LMS algorithm; including having a faster convergence speed for an automatic time-varying choice of the LMS step size parameter. The NLMS filter block is taken from the software package MATLAB/SIMULINK can implement an adaptive FIR filter using NLMS filter algorithm.

The NLMS filter block estimates the correct value of filter weights or coefficients. These filter weights or coefficients values are needed to minimize the error $e(n)$ between the output signal $y(n)$ and the desired signal $d(n)$. This can be implemented by using NLMS filter and simulated waveforms are given in figure.1.3. The output of filter is equal to the desired signal if the noisy signal is completely (i.e. when error is zero) filtered from the input signal.

The signal that requires filtering is connected to the input port of NLMS filter. The desired signal $d(n)$ is connected to the desired port of NLMS filter. The output port of filter outputs the filtered input signal, which is the correct estimate of the desired signal. The error port gives the difference between output signal and the desired signal. This is indicated in the NLMS algorithm using LMS toolbox as shown in figure.1.3.

The NLMS filter algorithm is defined by the following equations:

$$y(n) = w(n-1)^T u(n) \quad (18)$$

$$e(n) = d(n) - y(n) \quad (19)$$

$$w(n) = w(n-1) + f(u(n), e(n), \mu) \quad (20)$$

The weight update function for the normalized LMS algorithm is defined in the below equation,

$$f(u(n), e(n), \mu) = \frac{\mu e(n) u^*(n)}{(\epsilon + u^T(n) u(n))} \quad (21)$$

Where, the variable n -the current time index, $u(n)$ -the vector of buffered input samples at step n , $u^*(n)$ -the complex conjugate of the vector of buffered input samples at step n , $w(n)$ -the vector of filter weight estimates at step n , $y(n)$ -the filtered output at step n , $e(n)$ -the estimation error at step n , $d(n)$ -the desired response at step n , μ -the adaptation step size. ϵ - A small positive constant in order to avoid division by zero when the values of the input vector are zero or close to it. Hence, the instability due to division by zero is avoided [20].

The filter length parameter must be specified for the length of the filter weights vector. The step size parameter corresponds to μ in the equations. For convergence of the normalized LMS equations, μ is ($0 < \mu < 2$). All the LMS-like algorithms have a step size, which determines the amount of correction that is done as the filter adapts from the one iteration to the next. For this, the appropriate step size is not always easy; a step size that is too small will obstruct the convergence speed and accuracy, while that is too large may cause the filter to diverge and the resultant filter might not be stable. The filter design toolbox includes algorithms to determine the maximum step size allowed for ensuring the convergence. The first value of step size is the value needed for the filter coefficients of mean value to converge, while the second step size is the value needed for the mean squared filter coefficients to converge. Thus, the range of step size is from first value to second value. However, choosing a large step size results in large variations from the convergence values, so we choose smaller step size from first value to second value of step-size range. Here, we select μ is from $0 < \mu < 2$ by considering all filter parameters for the accurate convergence. The value of μ is greater than 2 produces high frequency ripples in final desired output. The value of μ defaults to 1.

To filter the noisy error signal “ u ”, which is the output signal of error detector for known BLDC motor parameters. It is specified to the input port of NLMS filter. The reference speed signal “ d ” is set as the desired signal to the adaptive filter, while “ y ” is necessary speed signal as the output signal in this filter setup. NLMS filter also estimates the filter weights “ w ” by normalized least mean square (NLMS) algorithm. The output of the filter, “ y ” will attempt to give “ d ” as best possible the desired signal.

This will be realized in an algorithmic procedure as exposed in figure.2.1. This describes the flowchart for NLMS adaptive algorithm to acquire the value of actual speed value of BLDC motor with defined loading condition. .

NLMS filter assigns the speed signal from the noisy error signal. This speed value is provided to facilitate the correct estimation of position information for actual motor running condition. By integration of speed signal gives the position evaluation curve for the computation of rotor position function $f_a(\theta)$, $f_b(\theta)$ and $f_c(\theta)$ making the block. Hence, back EMFs are calculated.

IV. CLOSED LOOP MODEL OF BLDC MOTOR WITH NLMS FILTER

Figure.2.2 offers closed loop proposed model of BLDC motor. The complete simulation model of PMSBLDC motor is exposed in Figure.2.2. The proposed simulation model has a flexible construction. The simulation has many blocks.

They are BLDC motor currents block, three phase voltage source inverter (VSI) block, back EMFs block, electrical torque (Te) block and three phase position block, NLMS filter block, hysteresis current controller block [21]. Each main block has several sub-blocks. Some blocks are logical types and some blocks are refined with the provision that all initial conditions can be simply varied [22]. The simulation begins with a BLDC core block that makes instantaneous rotor angle in radians for all the necessary system's block for one cycle. On one occasion the loop is closed, the BLDC core block will be disconnected from the whole system and the motor will put up with receiving phase voltages from the connected motor controller using NLMS filter and 3-phase VSI inverter.

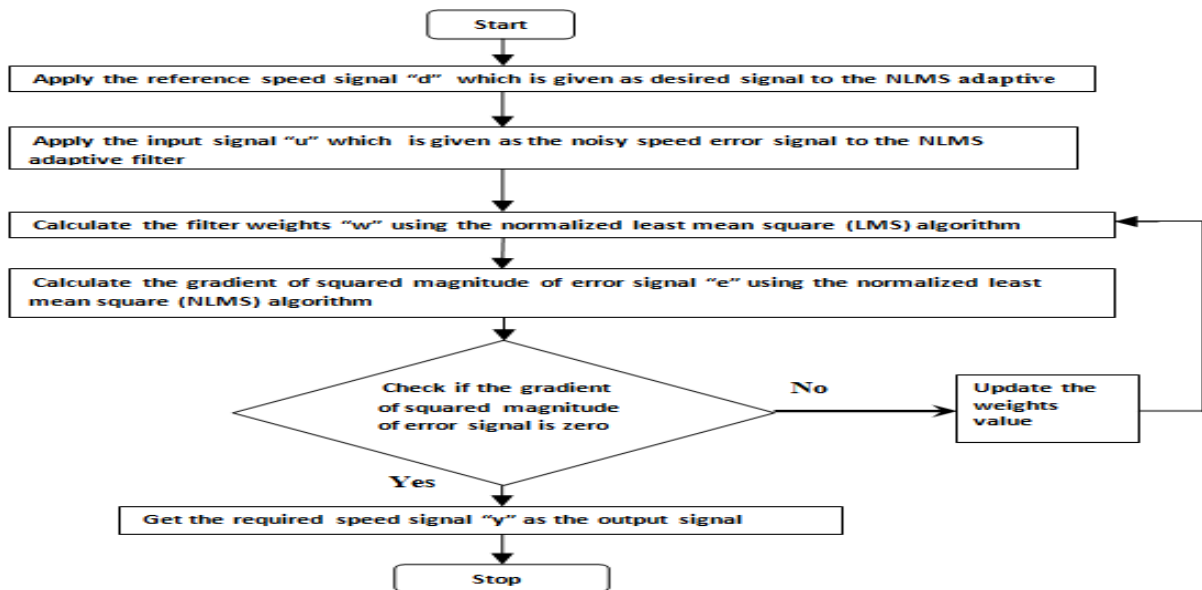


Fig.2.1 The flowchart for NLMS adaptive algorithm

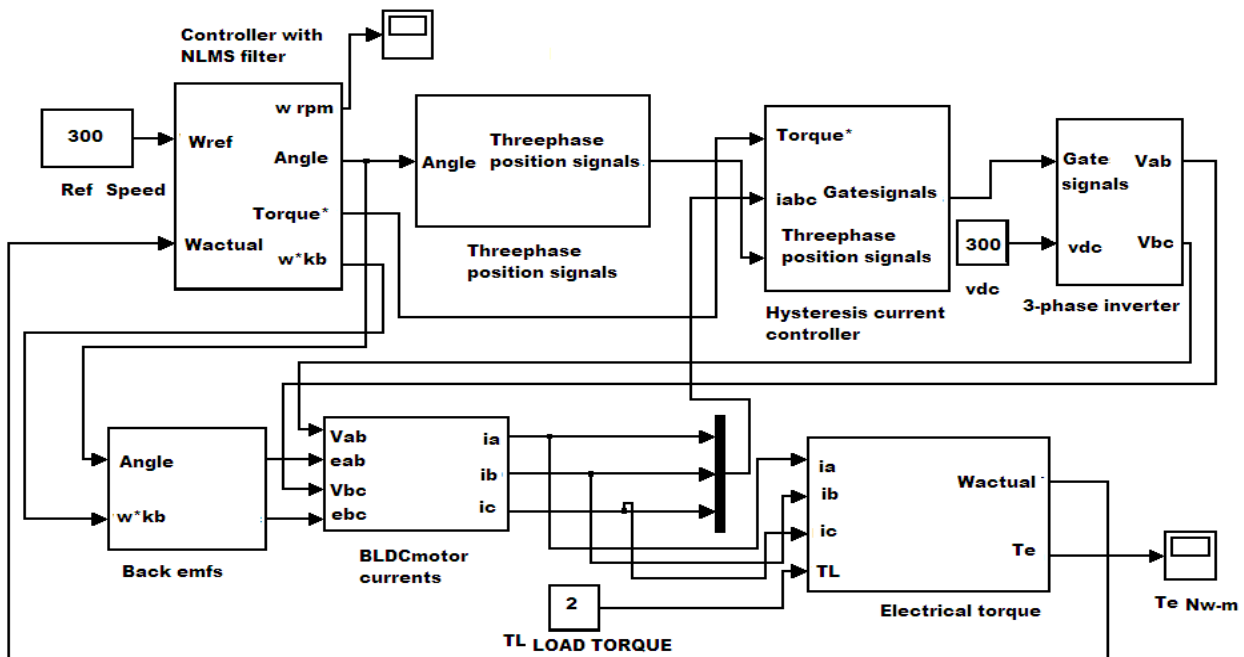


Fig.2. 2 Closed loop proposed model of BLDC motor

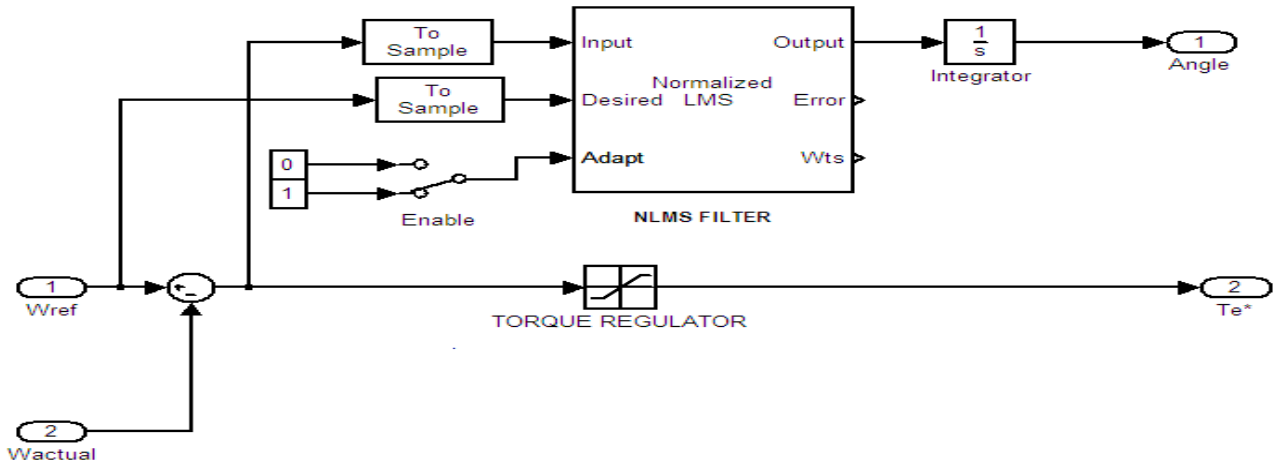


Fig.2.3 The block diagram for speed controller block with NLMS filter block

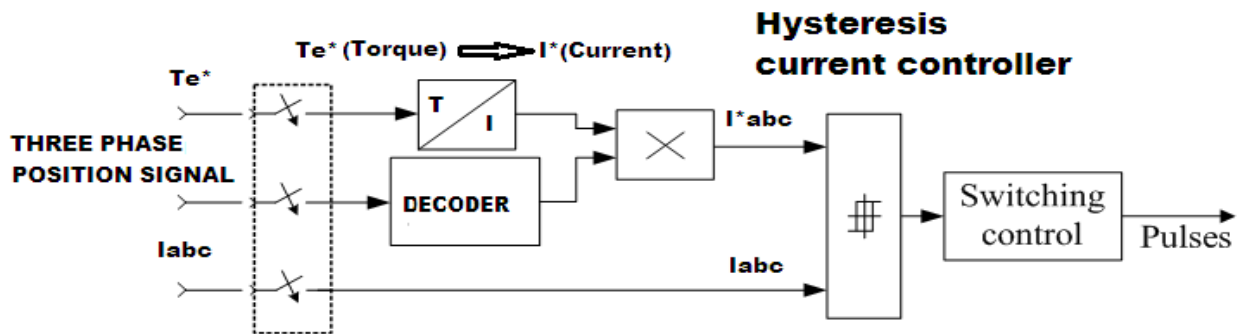


Fig. 4The block diagram of hysteresis current controller

Figure.2.3 demonstrates the block diagram for speed controller block with NLMS filter block for an invention of reference torque (T_e^*) signal. NLMS filter offers the reference torque signal in agreement with maximum torque limit values. By taking the angle signal which is the integration of necessary speed in rad/sec., coding table of position signals is resultant as the Hall Effect sensor signal sequence for 120-degree commutation of BLDC motor as exposed in Table.1.

Table 1 Coding table of position signals

Angle (θ)	Position signal A phase	Position signal B phase	Position signal C phase
0° to 60°	1	0	1
60° to 120°	1	0	0
120° to 180°	1	1	0
180° to 240°	0	1	0
240° to 300°	0	1	1
300° to 360°	0	0	1

Figure.2.4 illustrates the block diagram of hysteresis current controller. Hysteresis current controller makes gating signals for the three-phase inverter. Hysteresis-band current controller PWM is fundamentally an instantaneous feedback current control method of PWM in which the exact current frequently tracks the command current within set hysteresis-band [23]. Thus, by regulating the current, hysteresis current controller constructs a very good quality of quasi-square waveforms. By using, gating signals, three-phase inverter builds three-phase input voltages for six-step operation of BLDC motor. In this closed loop model, position signal acquired by normalized LMS filter gives the

precise assessment of gating signal sequence for the generation of three phase supply voltages to the BLDC motor with reduced ripple content as like hall signals for certain load condition and motor parameters. Duty cycles of three phase voltages are properly varied for the change of reference speed and load provision. Hence, this model can be easily executed for one open loop and closed loop operation.

V. SIMULATION RESULTS

In this paper, simulation results are gained by suitably selecting the values of normalized LMS filter parameters. The normalized LMS filter parameters are taken as follows: filter length=32, step size=0.1, leakage factor=1 and the initial value of filter weights are taken as zero. NLMS parameters need not be altered for each simulated result. At this point, the results are derived with BLDC motor parameters as given in Table 2.

The MATLAB/SIMULINK environment is used for the simulations. This paper ensures the robustness of the sensorless algorithm through the variations of speed and load. The dynamic performance of the BLDC drive under the load turbulence is analysed by a dynamic load of 0.5 N-m at 0 to 0.1 sec and 0.8 N-m at 0.75 sec to 1 sec to the motor while it runs at the speed of 100 rad/sec (Figures.3.1, 3.2, 3.3, and 3.4). Likewise, the dynamic performance of BLDC drive under load disturbance is tested by a dynamic load of 0 N-m at 0 to 0.1 sec and 3 N-m at 0.75 sec to 1 sec to the motor whereas it runs at the speed of 300rad/sec (Figures. 4.1, 4.2). Rotor position information attained from this proposed method is very similar to actual hall signals.

In this proposed work, using NLMS filter first utilized to start the motor from standstill condition at no-load or any other desired load. This type of operation is called as starting mode or aligning mode. Then, the motor is running with the same speed at any other preferred load in aligning mode. Hence, this mode of operation is called as “align then go”. By using this proposed model with NLMS filter, the motor is aligned for the required speed of operation by the proper generation of commutation gating signals.

Figure.3.1 and Figure.3.2 show simulated result of the generation of commutation signals for starting mode. The motor is running with the speed of 100 rad/sec during starting at 0.5 N-m load torque until the time of about 0.1 seconds. Hence, the motor is said to be in the “starting mode.” After which the motor is said to be in the “running mode” with loading transient of 0.8 N-m at 0.75 sec to 1 sec for the speed same of 100rad/sec as shown in Figure.3.3 and Figure.3.4 .

If the value of reference speed is varied and the duration of voltages applied to the motor is automatically varied to obtain the closed-loop control. This method of process of the sensorless scheme can be easily applied for starting the motor at any desired speed from rest condition at no-load or any other desired load in open loop control. After sensing the first commutation point, the motor is running through the same speed at any desired load in the closed mode of operation by the proper creation of commutation signal.

Hysteresis current controller appropriately designed for limiting the current values to safe values. Table.2 shows that parameters for PMBLDC motor are taken for the proposed work. Thus, torque and speed are controlled by a sensorless algorithm by means of the probably estimated speed with the time interval of commutation points.

Table 2 Parameters of BLDC Motor

Parameters	Value	Unit
Number of Poles(P)	4	-----
Rated speed	600	Rad/sec
Rating	5	HP
Resistance/phase(R_a)	1.2	ohms
Inductance /phase(L_a+M)	0.008	Henry
Back EMF constant(K_b)	0.1433	Volt/rad/sec
Moment of Inertia(J)	0.0198	Nw-m-sec ² /rad
Friction co efficient(B)	0.0012	Nw-m/rad/sec
Torque constant(K_t)	0.1433	Nw-m/Amp
Type of connection	star	-----

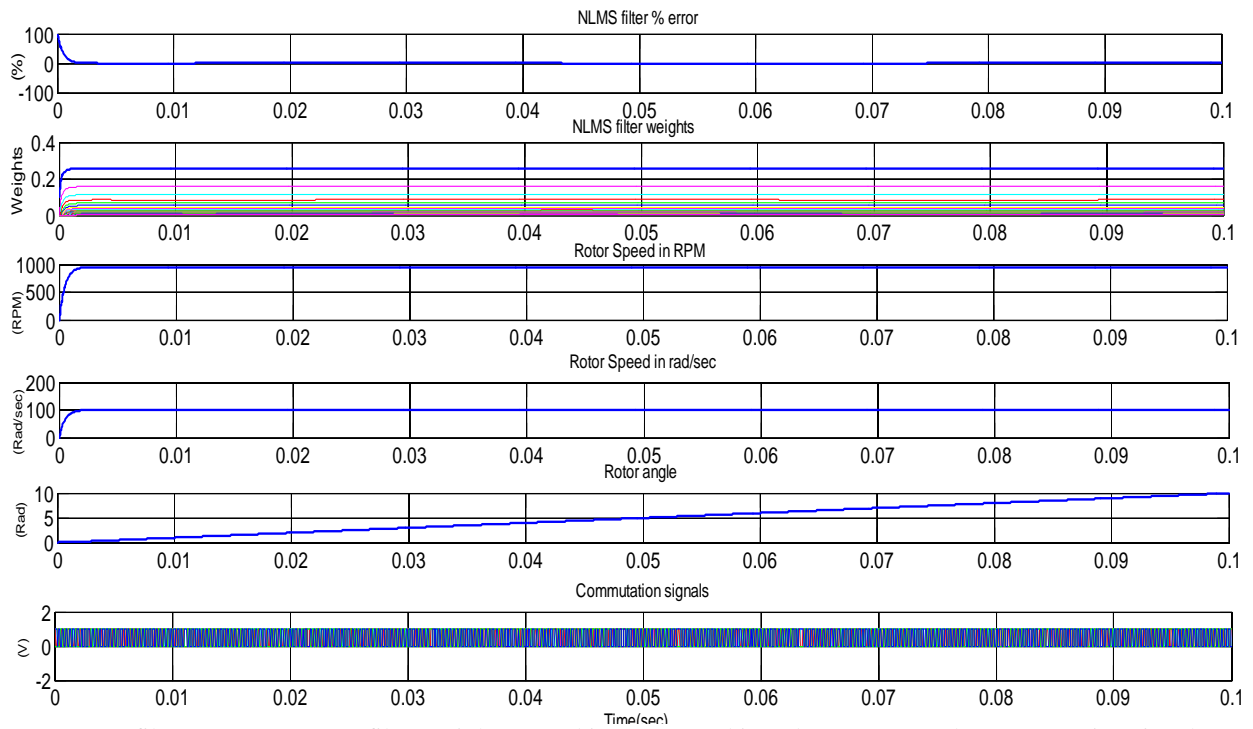


Fig.3.1 NLMS filter % error, NLMS filter weights, speed in rpm, speed in rad/sec, rotor angle, commutation signals (starting mode)

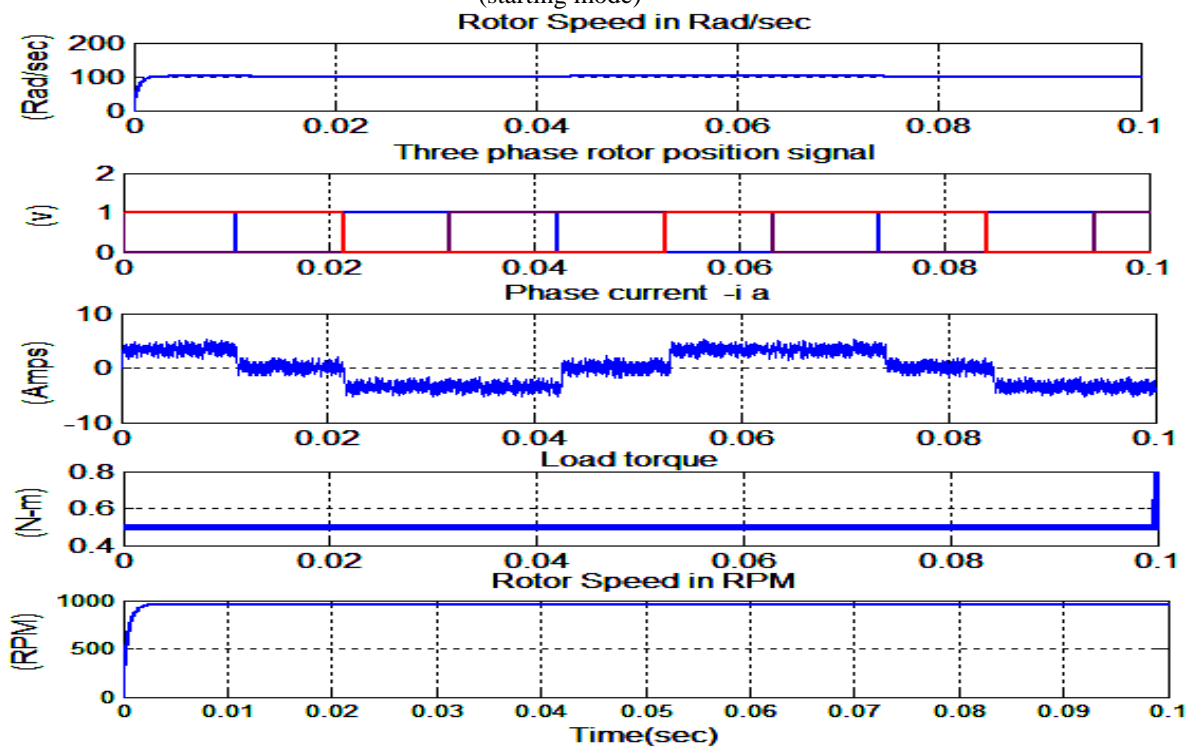


Fig.3.2 Speed in rad/sec, three phase rotor position signal, phase current- i_a , load torque, rotor speed in rpm (starting mode)

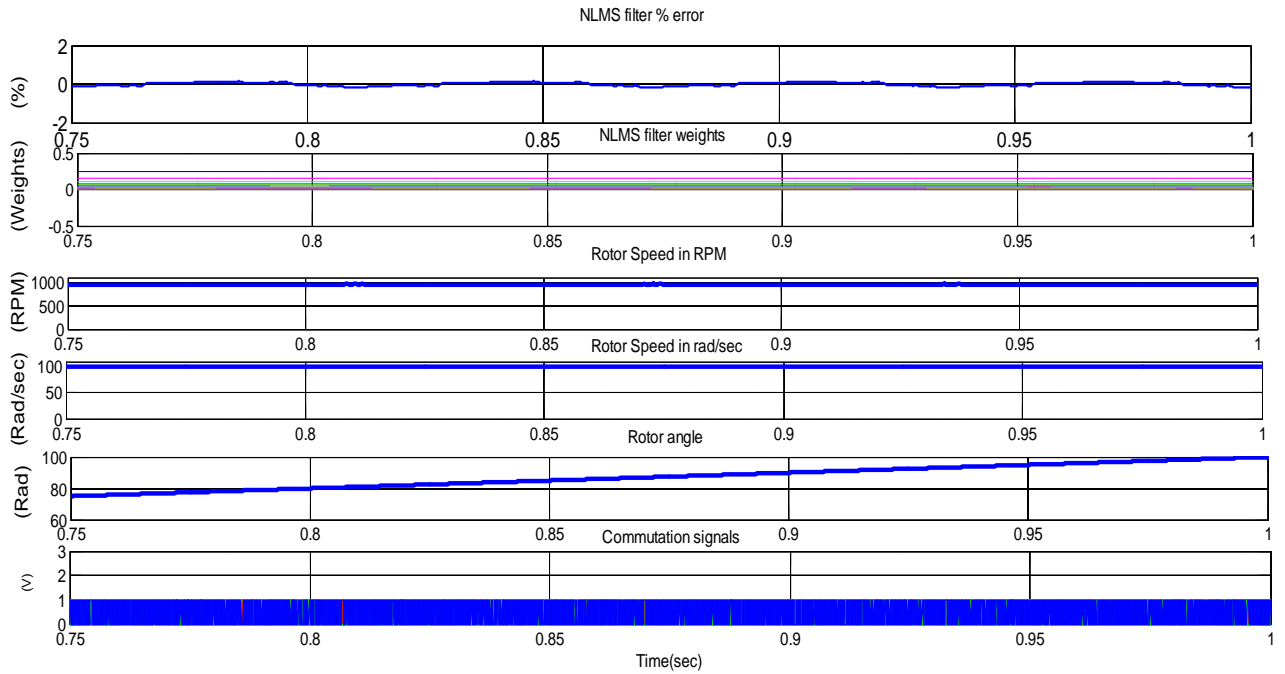


Fig.3.3 NLMS filter % error, NLMS filter weights, speed in rpm, speed in rad/sec, rotor angle and commutation signals (running mode)

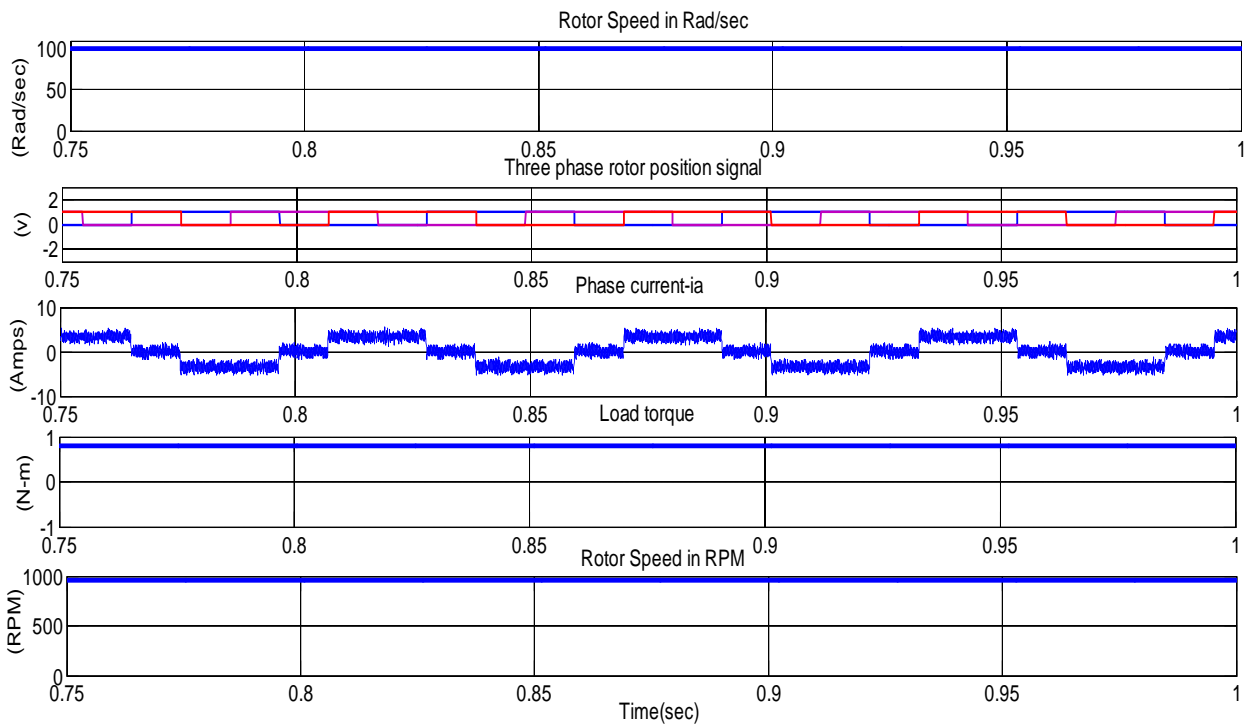


Fig.3.4 Speed in rad/sec, three phase rotor position signal, phase current-ia, load torque, speed in rpm (running mode)
 Fig.3. Simulated waveforms of motor for starting mode at $T_L=0.5N\text{-m}$ (0 to 0.1 sec) and for running mode at $T_L=0.8 N\text{-m}$ at 0.75 sec to 1 sec with a speed of 100 rad/sec

Fig.3 demonstrates the simulated waveforms of the motor for starting phase at $T_L=0.5\text{N-m}$, $t=0$ to 0.1 sec and a speed of 100 rad/sec. Figure.3.1 explains the simulated waveforms of NLMS filter % error, NLMS filter weights, speed in rpm, speed in rad/sec, rotor angle, and commutation signals. Here, speed in rpm, speed in rad/sec are simulated to calculate rotor angle .Figure.3.2 illustrates the simulated waveforms of speed in rad/sec, three-phase rotor position signal, phase current- i_a , load torque, speed in rpm. . Here, speed in rpm, speed in rad/sec are derived for checking load effect at the application of load torque $T_L=0.5\text{N-m}$.Figure.3 explains that how NLMS filter employed to generate commutation signal during starting phase or starting mode. Then, motor's parameters such as current, three-phase position signals are simulated for the same speed of 100 rad/sec at starting phase. NLMS filter affords the actual speed of 100 rad/sec by using a proper estimation of filter weights. Percentage error is reduced from maximum to zero value in step-by-step procedure by following the steps given in the flow chart of Figure.2.1. Finally, rotor angle is simulated for 100 rad/sec at starting mode for evaluation of three-phase rotor position signal.

Figure.3.3 also demonstrates the simulated waveforms of the motor for running phase at load torque $T_L=0.5\text{N-m}$ to 0.8 N-m, $t=0$.75 sec to 1 sec and a speed of 100 rad/sec. Figure.3.3 explains the simulated waveforms of NLMS filter % error, NLMS filter weights, speed in rpm, speed in rad/sec, rotor angle, and commutation signals. Fig.3d illustrates the simulated waveforms speed in rad/sec, three phase rotor position signal, phase current- i_a , load torque, speed in rpm. Figure.3.3 and Figure.3.4 explains that how the NLMS filter employed to produce commutation signal during running phase or running mode. Then, motor's parameters such as current, three-phase position signals are simulated for the same speed of 100 rad/sec at running phase or running mode.

Figure.4 exhibits the speed in rad/sec, three phase rotor position signal, phase current- i_a , load torque, speed in rpm waveforms of the motor for starting mode and running mode with a speed of 300 rad/sec. Figure.4.1 demonstrates at $T_L=0$ N-m at 0 sec to 0.1 sec for starting mode. These simulations are brought to explicate the starting mode of sensorless operation procedure. Figure.4.2 shows at $T_L=3$ N-m, $t=0.75$ sec to 1 sec for running mode with a speed of 300 rad/sec. When the motor is started from rest condition with no-load, NLMS filter gives three phase position signal for angle derived with a speed of 300 rad/sec.The gating pulses and commutation points defined in this situation is known as starting mode or starting phase of the motor at no-load. After application of load torque $T_L=3$ N-m, there is a change in actual running speed of 300 rad/sec.But, in this running mode NLMS filter again furnishes the same commutation points for the speed of 300 rad/sec. Hysteresis current controller restricts the current in the safe limit. Thus, the motor is running through the same 300 rad/sec when the load torque varies from 0 N-m to 3 N-m.

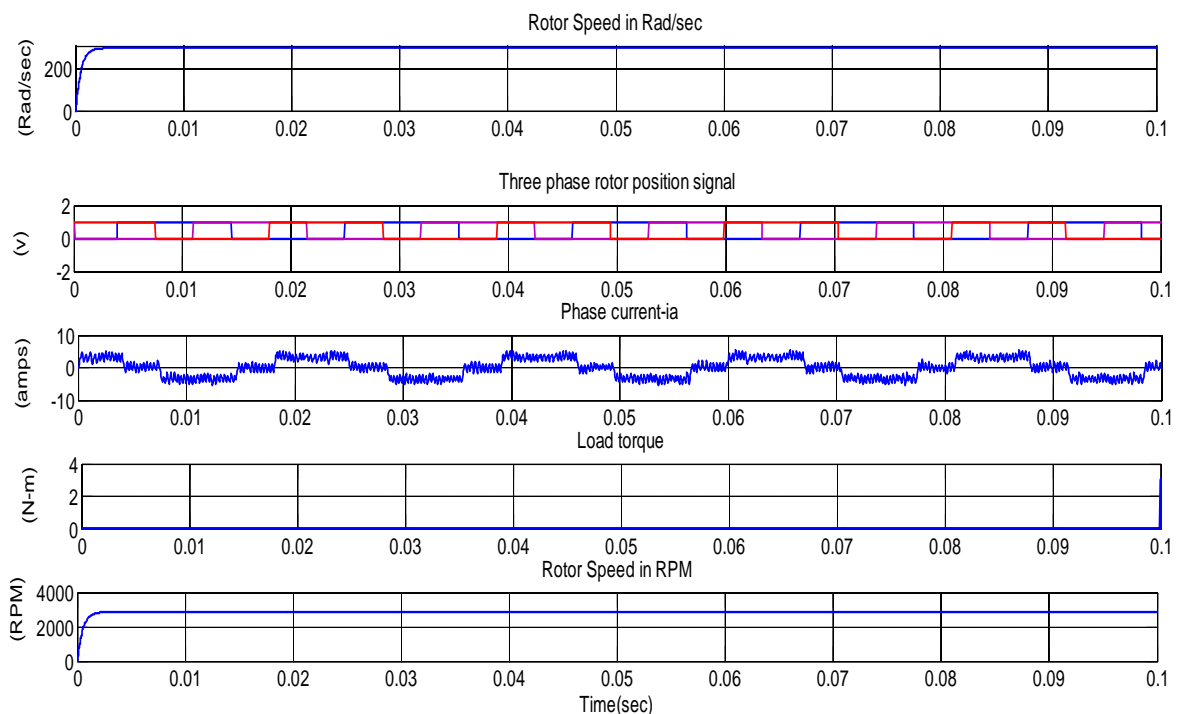


Fig.4. 1 Speed in rad/sec, three phase rotor position signal, phase current- i_a , load torque, speed in rpm

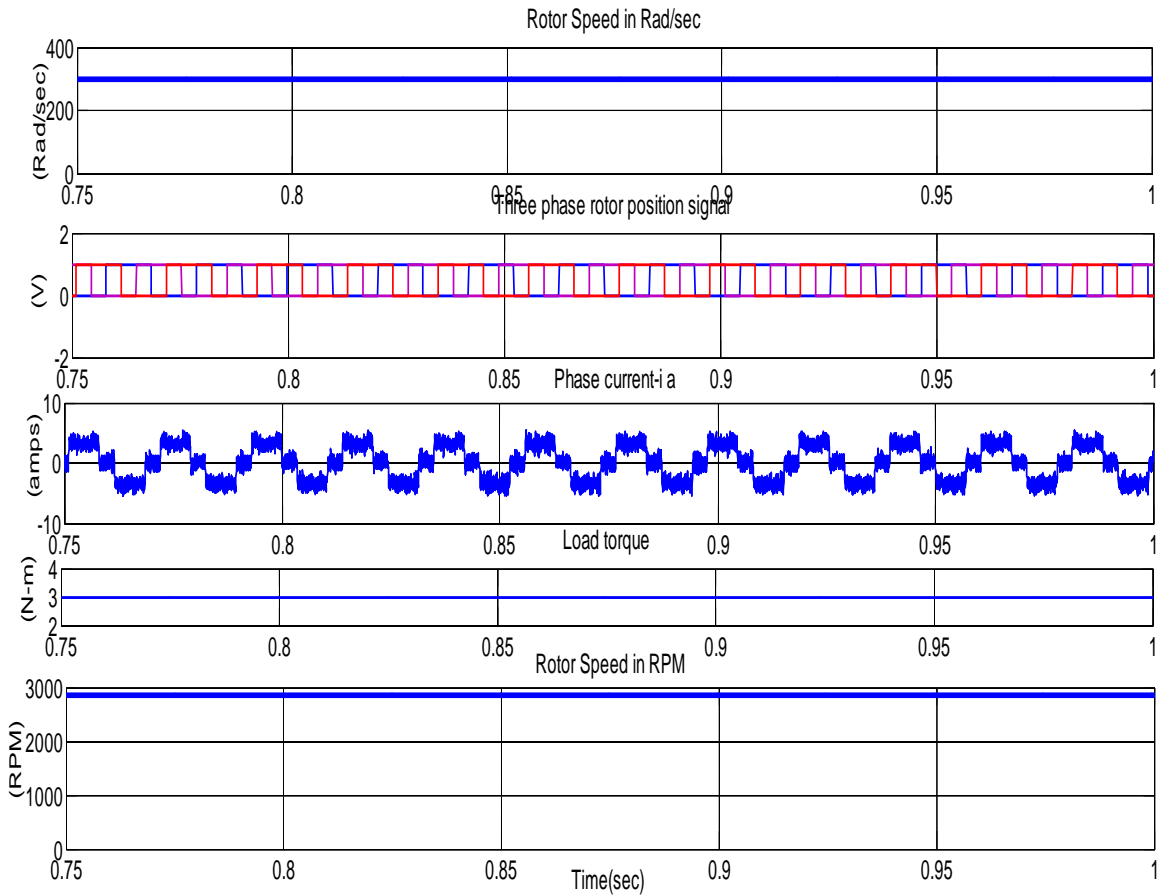


Fig.4. 2 Speed in rad/sec, three phase rotor position signal, phase current-ia, load torque, speed in rpm

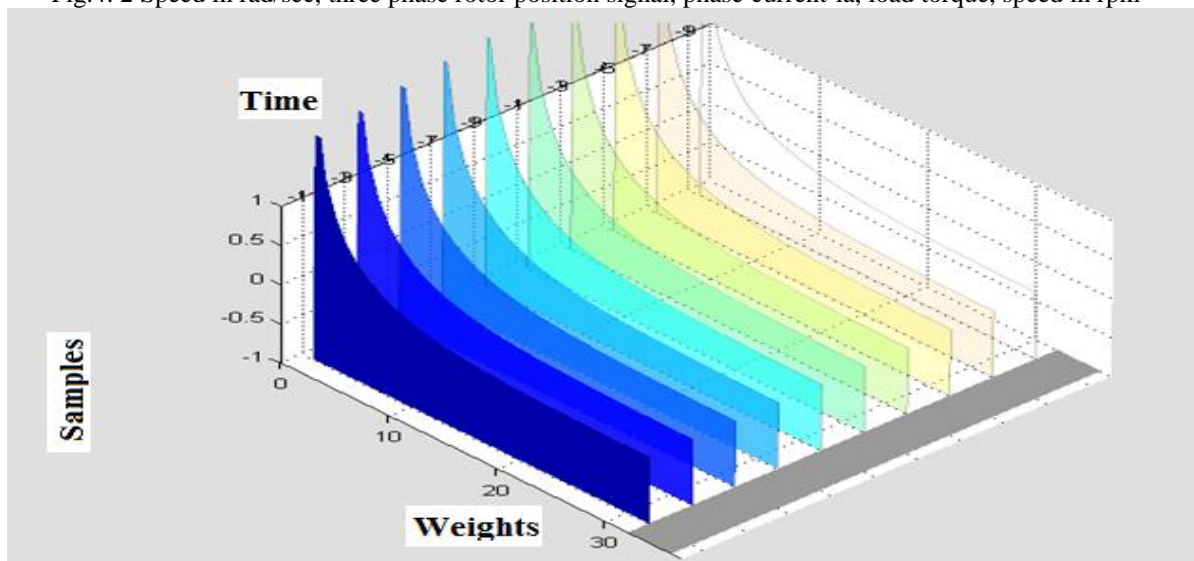


Fig.4.3 Weights output for various samples pulses at $T_L=0$ N-m for 300 Rad/sec and at $t=0.1$ sec using NLMS filter

Fig.4.Simulated waveforms of motor at $T_L=0$ N-m for starting mode and $T_L=3$ N-m for running mode for a speed of 300 rad/sec

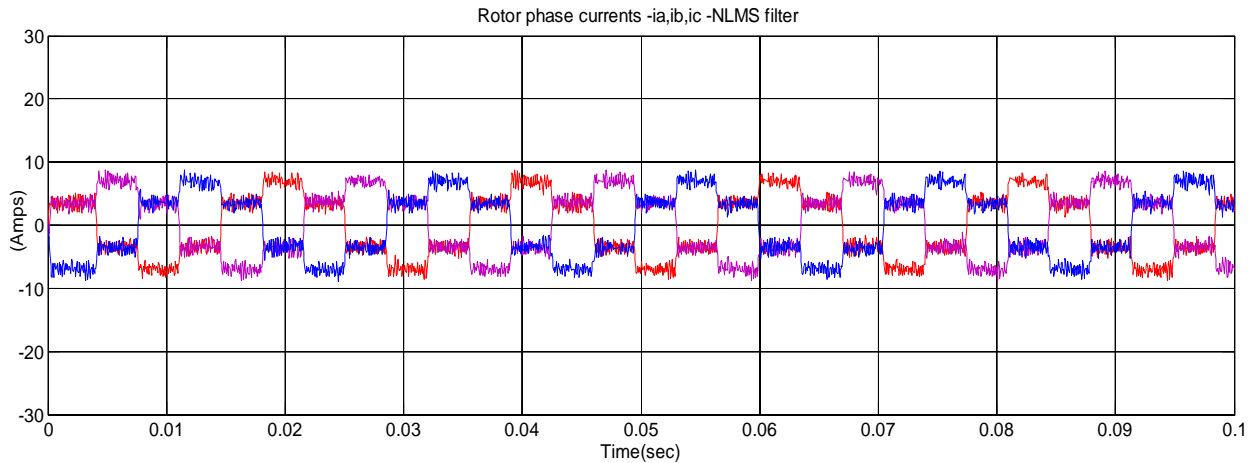


Fig.5.1 Three phase currents for NLMS filter controller

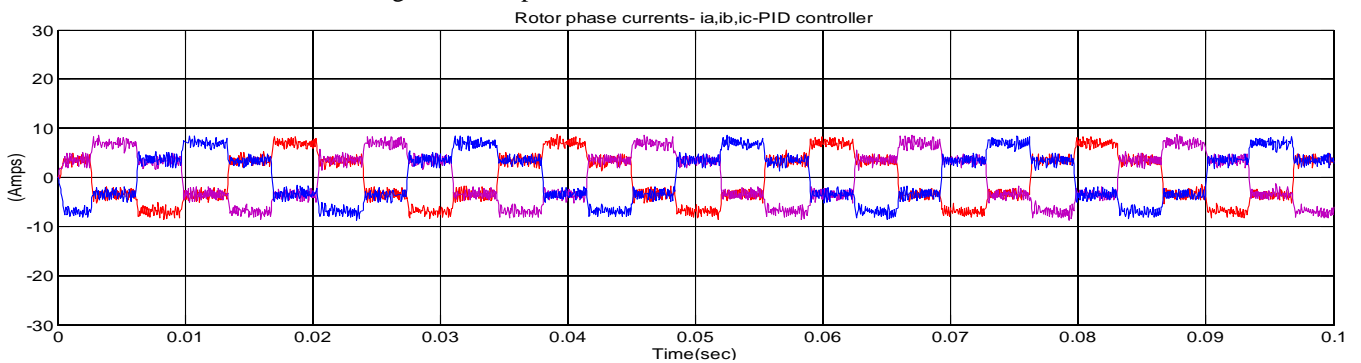


Fig.5.2 Three phase currents for PID controller

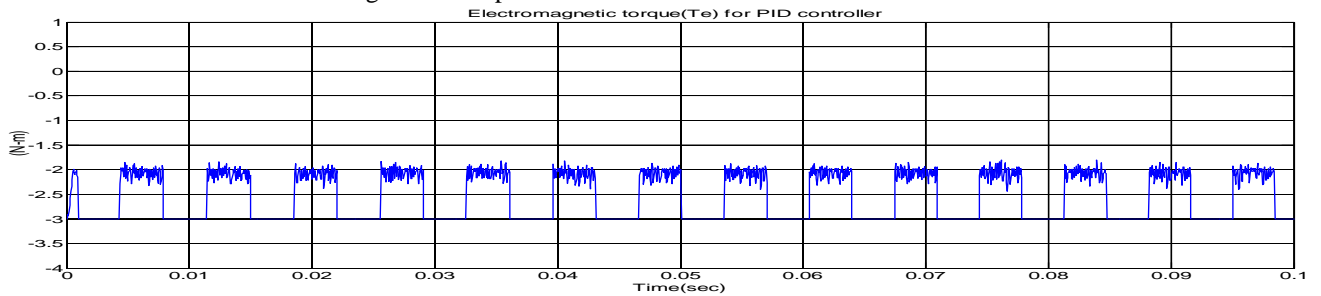


Fig.5.3 Electromagnetic torque waveform for PID controller

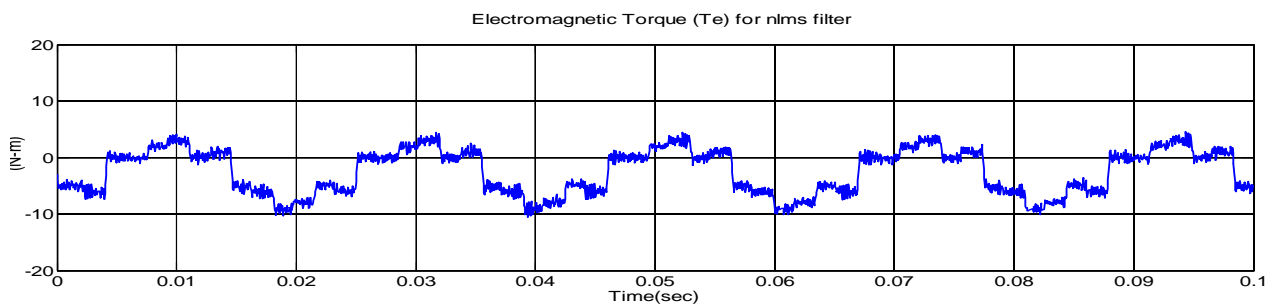


Fig.5.4 Electromagnetic torque waveform for NLMS filter controller

Fig.5. Simulated waveforms of motor three phase currents, electromagnetic torque for starting mode at $T_L=3$ N-m, 300 rad/sec

Figure.5 illuminates the simulated waveforms of motor three phase currents i_a , i_b , i_c , electromagnetic torque (T_e) for starting mode at $T_L=3$ N-m at 0 sec to 0.1 sec with a speed of 300 rad/sec. Figure.5.1 and Figure.5.4 furnish results for NLMS filter. Figure.5.2 and Figure.5.3 offer the results for PID controller. These are ensuing to calculate current ripples of PID controller and NLMS filter. PID controller allocates to give high current ripples than NLMS filter as given in Table 3.

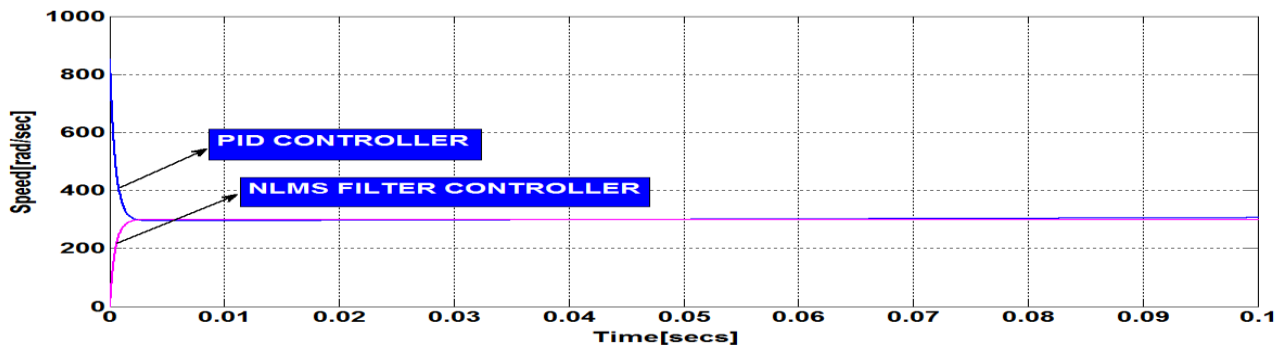


Fig.6.1 Speed curve of PID controller, NLMS filter controller for starting phase $T_L=3$ N-m with a speed of 300 rad/sec

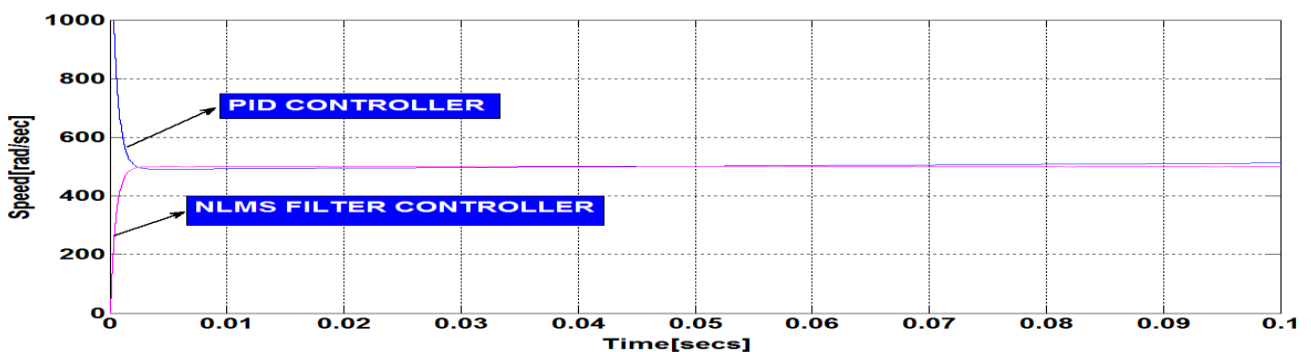


Fig.6.2 Speed curve of PID controller, NLMS filter controller for starting phase $T_L=5$ N-m with a speed of 500 rad/sec

Fig.6. Speed curve of PID controller, NLMS filter controller for starting phase

Figure.6 illustrates the simulation result of BLDC motor for speed curves of PID controller and NLMS filter controller for starting phase. Figure.6.1 shows result for $T_L=3$ N-m at 0 sec to 0.1 sec with a speed of 300 rad/sec. Figure.6.2 shows result for $T_L=5$ N-m at 0 sec to 0.1 sec with a speed of 500 rad/sec. These are results for the speed of 300 rad/sec and 500 rad/sec, which specify that the use of PID controller for speed control of BLDC motor drive is to be characterized by an overshoot during initial tracking mode or starting mode. This will lead to increase the current ripples and vibrations in the motor during running mode. The utilization of PID controllers for speed control of BLDC motor drive gives higher peak overshoot, steady state error and rise time than NLMS filter response. It is evident that speed tracking by using NLMS filter at all speeds is better than PID controller. All simulation results designate the fast and smoothness of NLMS filter response.

The robustness of this proposed method is checked for the NLMS filter initial set-up. Simulation results of Figure.4 are expanded by suitably altering the values of normalized LMS filter initial set-up parameters. The normalized LMS filter parameters are taken as follows: filter length=64, step size=0.2, leakage factor=1 and the initial value of filter weights are taken as zero. These results are derived with BLDC motor parameters as given in Table 2. The similar results are derived in the Figure.7 at $T_L=0$ N-m for starting mode and $T_L=3$ N-m for running mode and a speed of 300 rad/sec. Figure.7.3 gives weights output for various samples at $T_L=0$ N-m for 300 rad/sec and at $t=0.1$ sec using NLMS filter. The same 300 rad/sec speed curve is obtained for the change of filter initial set-up parameters. Hence; the robustness of proposed method is validated for the change of filter initial set-up parameters.

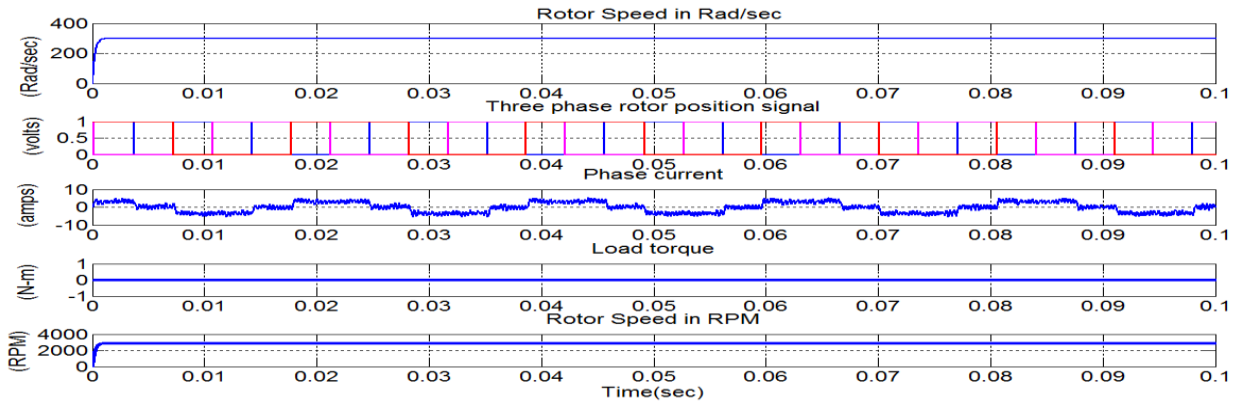


Fig.7. 1 Speed in rad/sec, three phase rotor position signal, phase current-ia, load torque, rotor speed in rpm

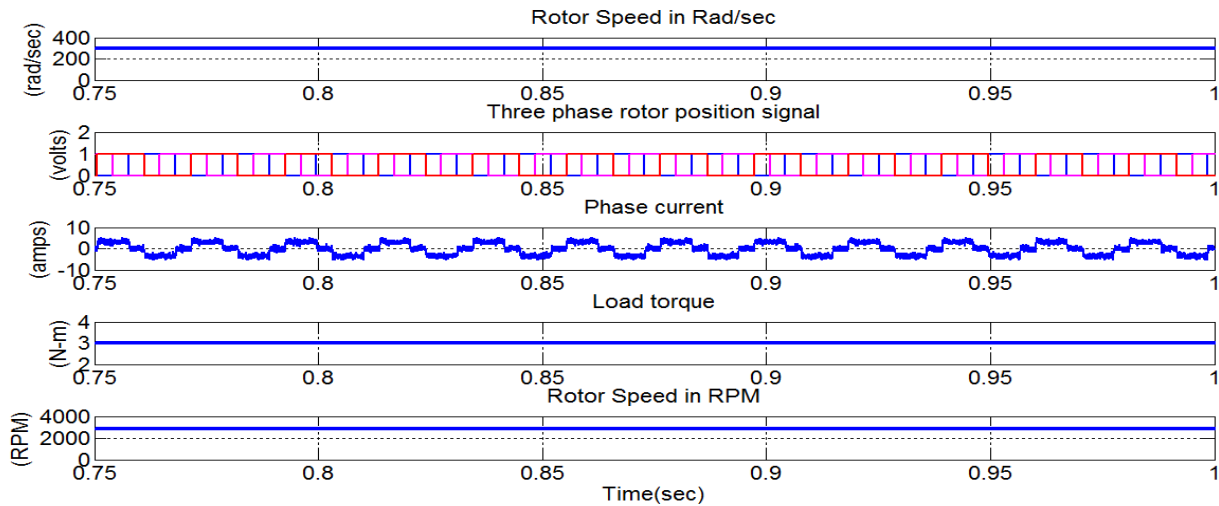


Fig.7. 2 Speed in rad/sec, three phase rotor position signal, phase current-ia, load torque, rotor speed in rpm

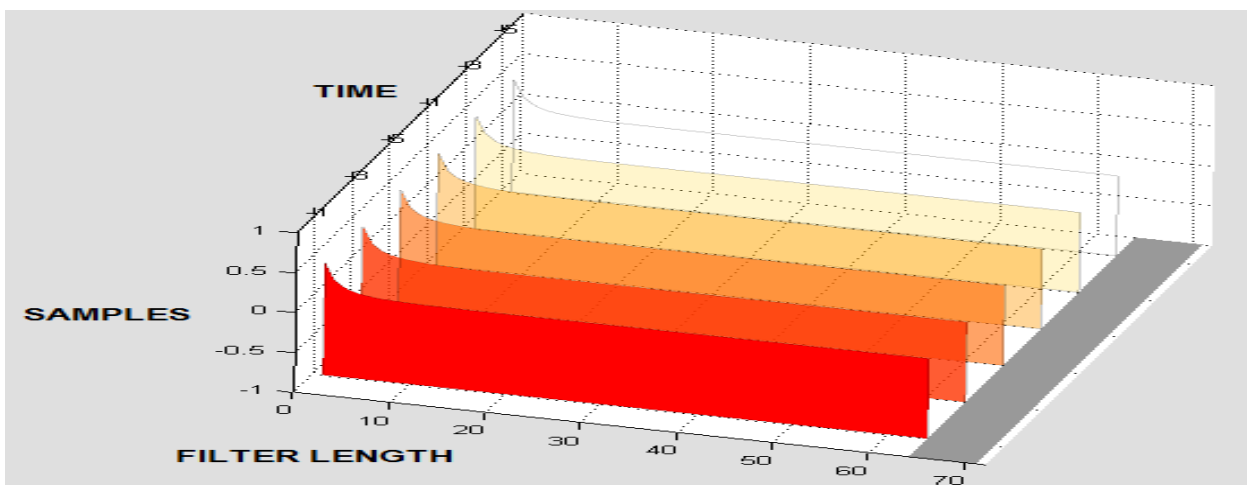


Fig.7. 3 Weights output for various samples at $T_L=0$ N-m for 300 rad/sec and at $t=0.1$ sec using NLMS filter

Fig.7. Simulated waveforms of motor for starting mode and $T_L=3$ N-m for running mode and a speed of 300 rad/sec

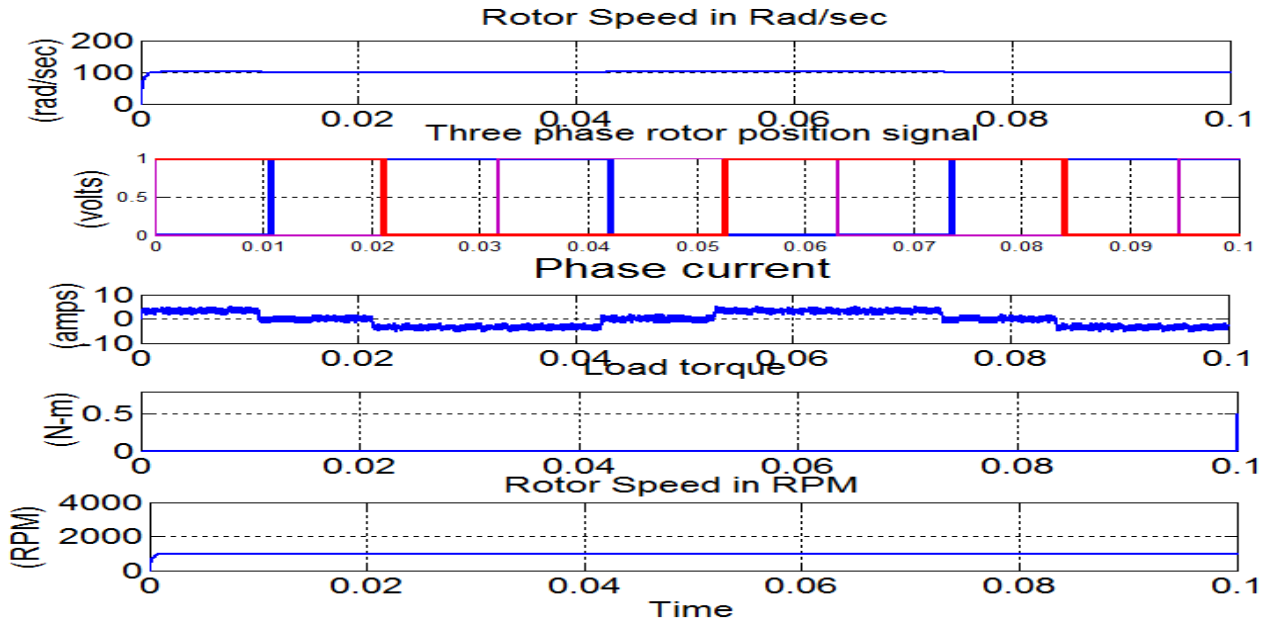


Fig.8.1. Speed in rad/sec, three phase rotor position signal, phase current-ia, load torque, rotor speed in rpm (starting mode)

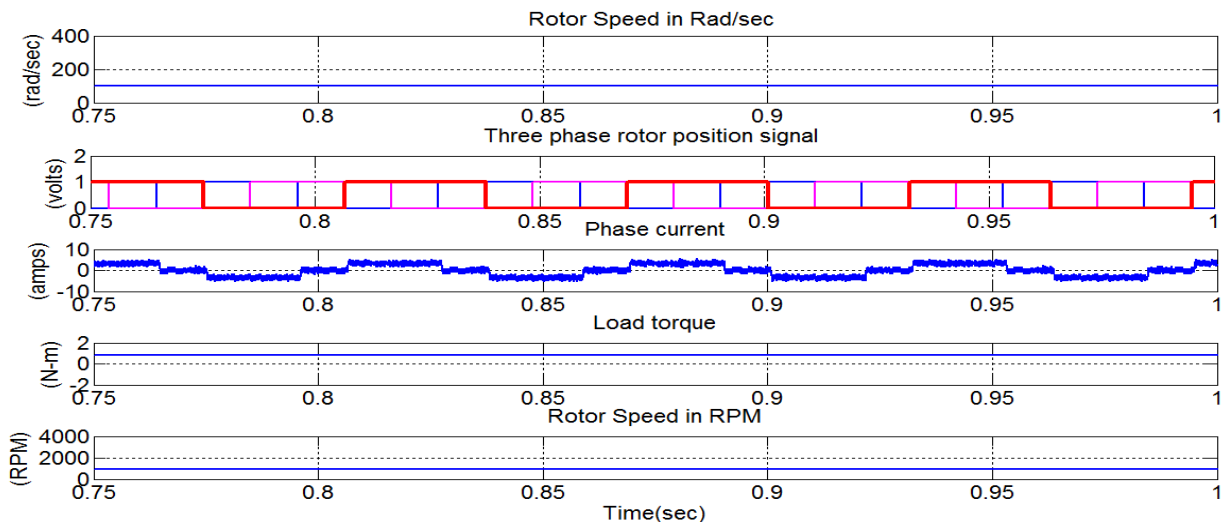


Fig.8.2 Speed in rad/sec, three phase rotor position signal, phase current-ia, load torque, rotor speed in rpm (running mode)

Fig.8. Simulated waveforms of motor for starting mode at $T_L=0.5\text{N-m}$ (0 to 0.1 sec) and running mode at $T_L=0.8\text{ N-m}$ at 0.75 sec to 1 sec with a speed of 100 rad/sec

Now, the robustness of the proposed method is checked for BLDC motor parameter variations. The following BLDC motor parameters are changed into consideration that inductance /phase (L_a+M) =0.006 Henry, resistance/phase (R_a) =0.5ohms, moment of inertia (J) =0.01455 N-m-sec²/rad, friction co efficient (B) = 0.0018 N-m/rad/sec. Figures.8.1, 8.2 shows the simulation results of starting and running mode of operation .The change of motor simulation results actually compared with simulation results of Figure.3. The same speed of 100 rad/sec is obtained using the same initial set up of NLMS filter parameters .From this, we observed that this proposed method is well suitable for any change of motor's parameter.

Table 3 The performance results of conventional PID controller, NLMS filter controller for 300 rad/sec with 3 N-m loads

Speed with load torque	300 Rad/sec with load torque of 3 N-m at time t=0.1sec	
Type of controller	PID controller	NLMS filter controller
Current ripples (%)	42.85	28.57
Rise time(sec)	3.5×10^{-3}	1.11×10^{-3}
Peak overshoot (%)	267	0.0
Steady state error (%)	2	0.06
%THD of rotor three phase position signal	49.68	42.85
%THD of phase current signal	48.04	39.47

Table 3 exhibits the performance of the BLDC motor drive with NLMS filter and PID controllers at 300 rad/sec with 3 N-m loads. PID controller parameters are allocated by $K_p=0.5$, $K_i=5$, $K_d=0.0005$. Usually, PID controller parameters are well agreed by trial and error and current is controlled via hysteresis current controller. The BLDC motor with NLMS filter attains the reference speed quickly without any overshoot. The step commands are captured with almost zero steady state error and load disturbances are entirely rejected. The load variations of the motor are literally well deal with nonlinearity performance.

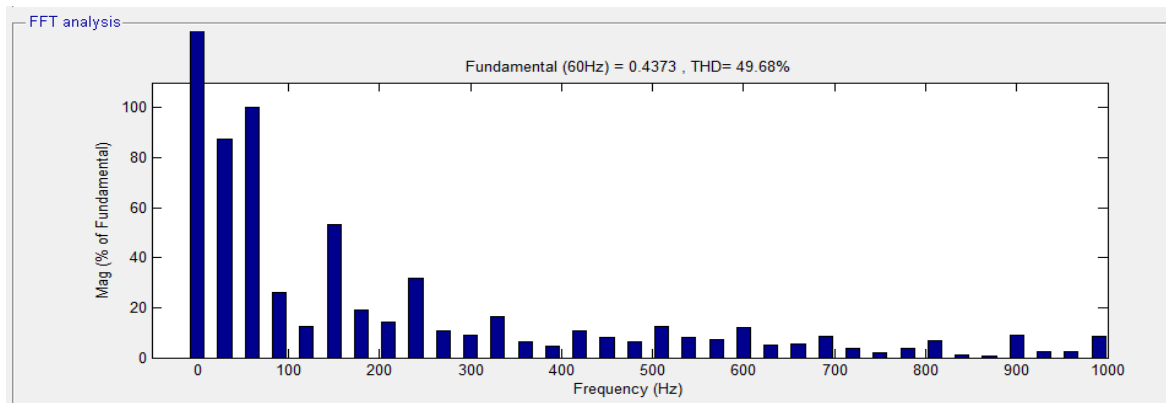


Fig.9.1 %THD of rotor position signal of PID controller for 300 rad/sec at load torque of 3 N-m

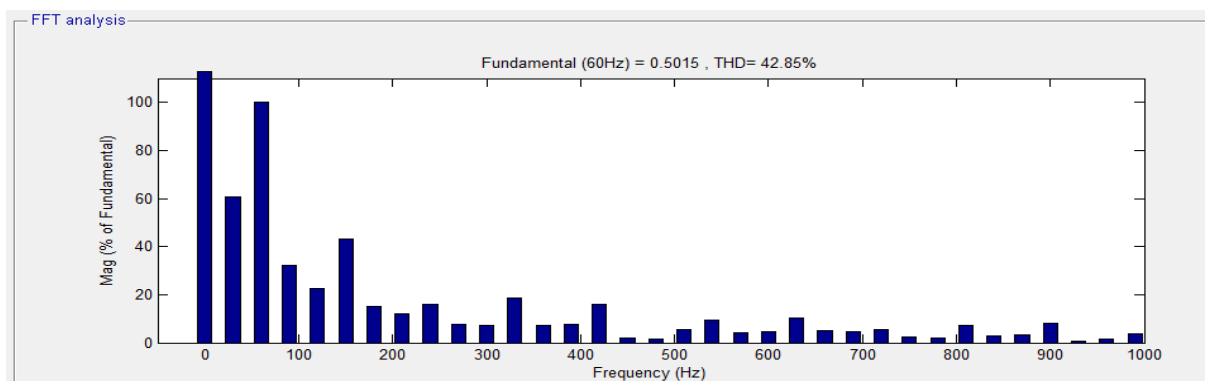


Fig.9.2 %THD of rotor position signal of NLMS filter controller for 300 rad/sec at load torque of 3 N-m

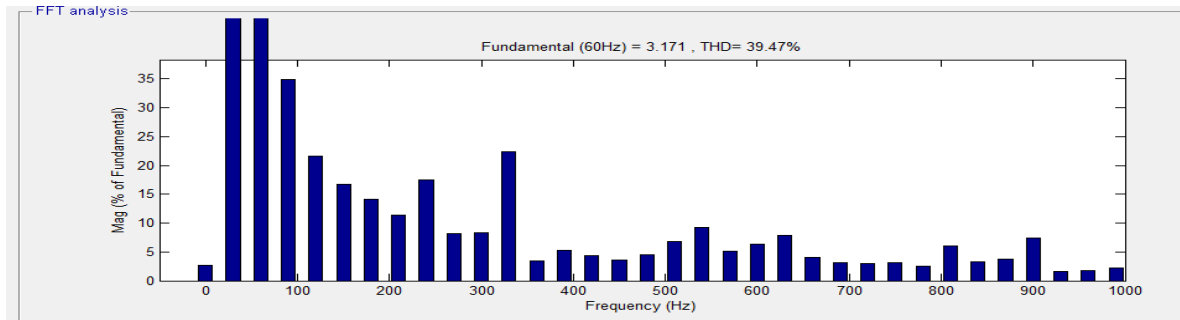


Fig.9.3 %THD of phase current signal of NLMS filter controller for 300 rad/sec at load torque of 3 N-m

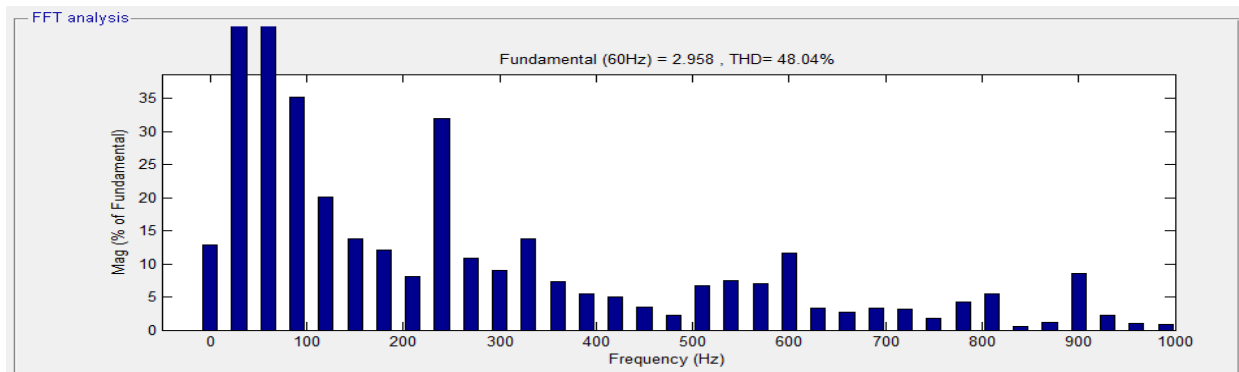


Fig.9.4 %THD of phase current signal of PID controller for 300 rad/sec at load torque of 3 N-m
Fig.9. %THD of rotor position signal, phase current signal of NLMS filter controller and PID controller

Figure.9 illustrates %THD of rotor position signal, phase current signal of PID controller and NLMS filter controller for 300 rad/sec at load torque of 3 N-m. Figure.9.1 denotes %THD of rotor position signal of PID controller for 300 rad/sec at load torque of 3 N-m. Figure.9.2 indicates %THD of rotor position signal of NLMS filter controller for 300 rad/sec at load torque of 3 N-m. Figure.9.3 implies %THD of phase current signal of NLMS filter controller for 300 rad/sec at load torque of 3 N-m. Figure.9.4 shows %THD of phase current signal of PID controller for 300 rad/sec at load torque of 3 N-m. Table 3 displays the functional results of conventional PID controller, NLMS filter controller for 300 rad/sec with 3 N-m load at time t=0.1sec. From the results of two methods of assessment, it is clear that NLMS filter gives less % of total harmonic distortion (THD) for rotor position signals and phase current signals.

VI. HARDWARE IMPLEMENTATION OF PROPOSED MODEL

In this proposed model, the hardware set-up consists of a BLDC motor, FPGA control system, three phase inverter. The speed controllers put into practice in VHDL module with Xilinx 9.1/FPGA hardware. It is a reference point control with the desired speed of the motor. Complete VHDL code is generated for closed loop proposed model is given in figure.2.2. The desired speed of motor on actual loading is applied to using NLMS filter block is given in figure.2.3. This is implemented by VHDL code generation of NLMS filter algorithm as shown in figure.10.1. The desired speed is given as 0012Ch in hexadecimal for 300 rad/sec with a load torque of 3 N-m, step size of 0420h as shown in figure.10.1. From this desired speed as the output speed of motor, angle is calculated as 0.00171887 in degrees with a input speed of 100 rad/sec (0064h in hexadecimal). This angle in degrees used to give a total position signal for three phases (001) a, b, c by taking (Table .1) coding table of position signals. This is implemented by VHDL code generation and given in figure.10.2. Finally, for actual running of 300 rad/sec speed; there are six non-zero gating signals for the two-phase control method, which are positioned at 60 electrical degrees separately from each other are formed. The first commutating signal is derived as (gate1gate2gate3gate4gate5gate6) 100001 as shown in figure.10.4. Thus, six PWM signals 001001, 011000, 010010, 000110, 100100 can be generated for the inverter operation using VHDL code implementation. Duty cycle of PWM signals correctly estimates the actual running speed of 300 rad/sec.

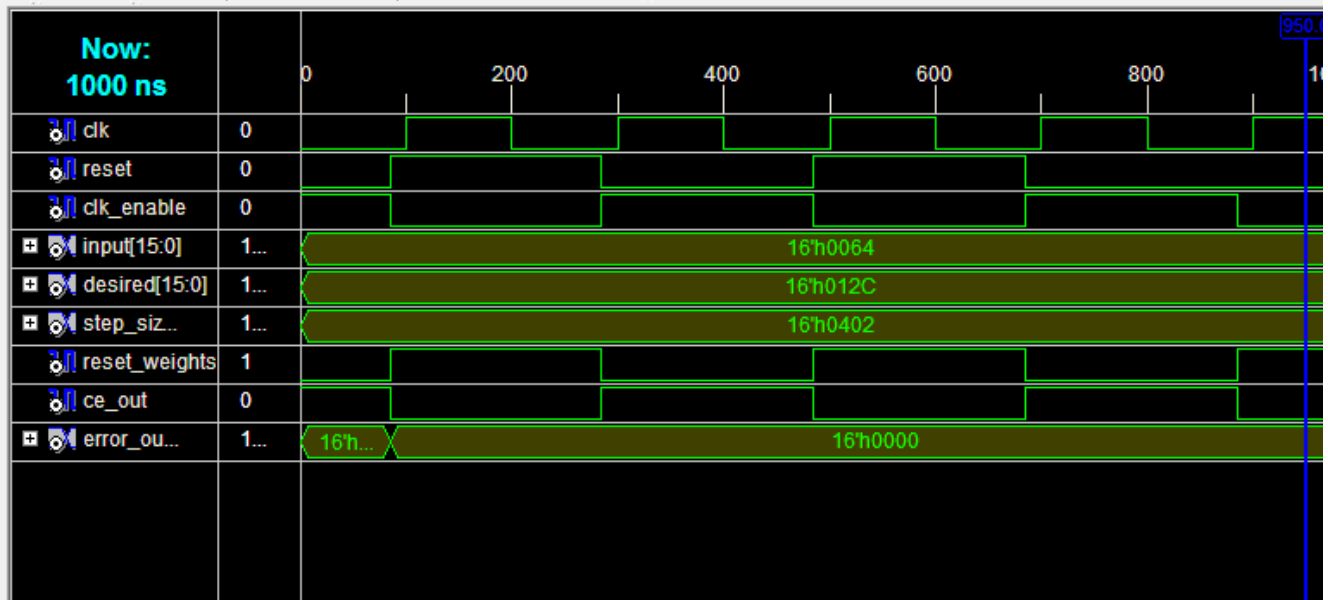


Fig.10.1 Experimental simulation of NLMS filter algorithm

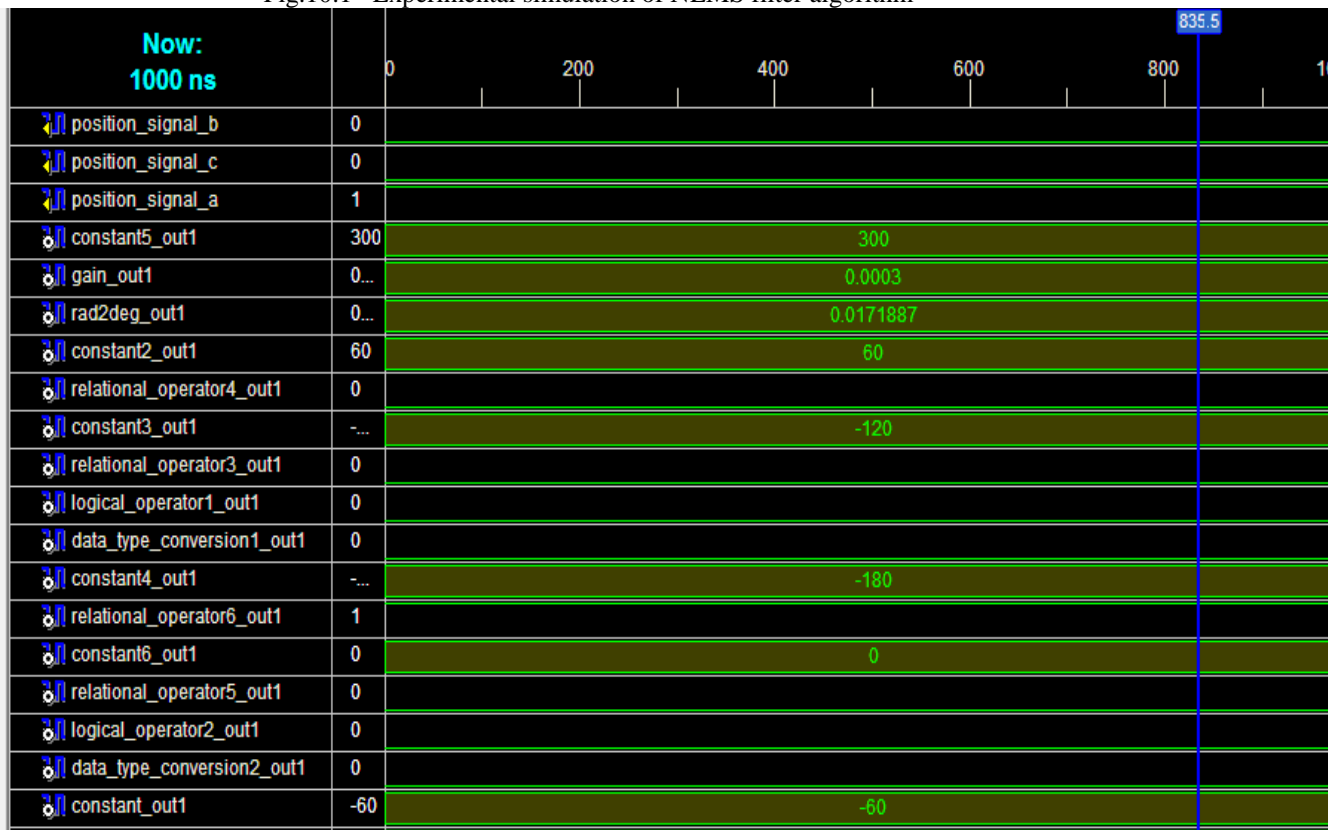


Fig.10.2 Experimental simulation of angle and total rotor position signal

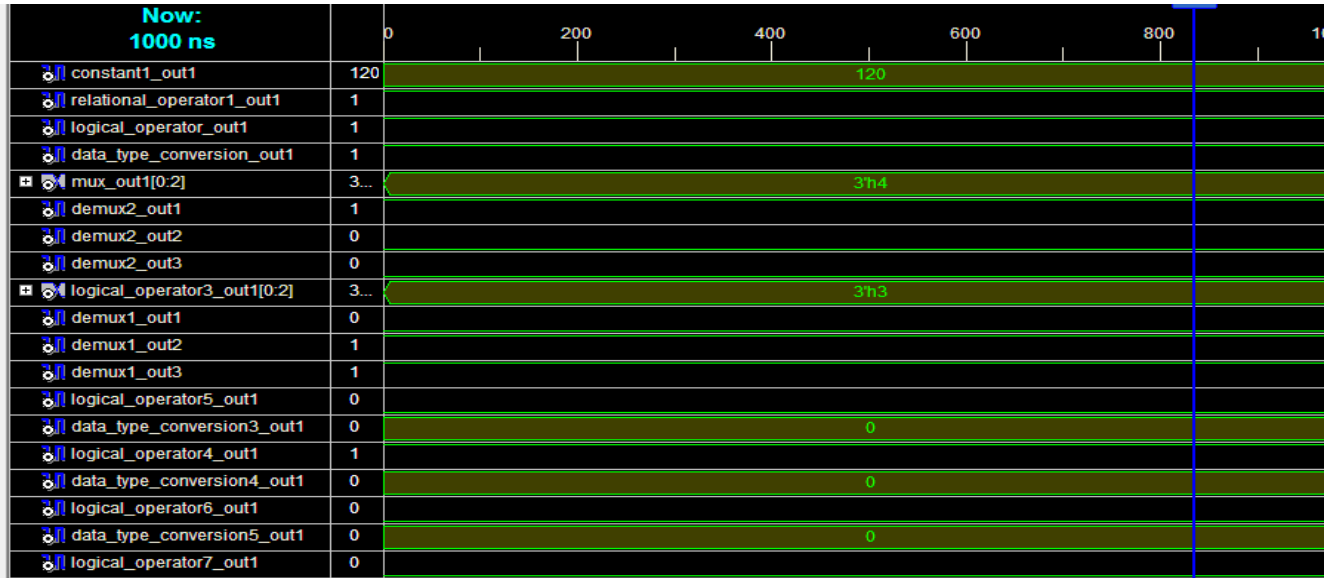


Fig.10.3 Experimental simulation of commutating signal for first six-step operation



Fig.10.4 Experimental simulation of commutating signal for first six-step operation

Fig.10. Experimental simulation of NLMS filter algorithm, angle and total rotor position signal, commutating signal for 300 rad/sec at load torque of 3 N-m

VII. CONCLUSION

This paper offered a new method to the sensorless control of the BLDC motor drives using the NLMS filter. The actual rotor position for the machine speed can be predictable accurately even in transient state as well as in steady state. This novel sensorless method can be achieved without using complicated design of additional circuits. This method can determine precise commutation pulse even in transient state as well as in steady state. This method detects the rotor position effectively over a full speed range for any low and high-speed values. This paper can be easily implemented for industry application by using simple error-reducing algorithm. Desired performance characteristics of BLDC motor are simulated and analysed under various loaded conditions. Commutation gate signal generation in this method is very liable for very low torque and voltage ripples. The simulation and experimental results successfully confirmed the validity of the developed sensorless drive technique using NLMS filter.

**VIII. FUTURE SCOPE**

The future scope of this paper is that the developed sensorless drive method is to be extended by using recursive least squares (RLS) adaptive algorithm. The simulation and experimental results can be acquired by using recursive least squares (RLS) adaptive algorithm.

REFERENCES

- [1] K.P., Pillay, R., Krishnan, "Modelling, Simulation and Analysis of Permanent-Magnet Motor Drives, part-II: the brushless DC motor drives", IEEE Trans. on Industry Applications, vol. 25, pp.274-279, March/April 1989.
- [2] Pragasen Pillay and Ramu Krishnan, "Application Characteristics of Permanent Magnet Synchronous and Brushless DC Motors for servo drives", IEEE Trans. on Industry Applications, vol. 21, no. 5, pp.987-996, September/October 1991.
- [3] P., Damodharan, R., Sandeep.K., Vasudevan, "Simple position Sensorless starting method for brushless DC motor", IET Electric Power Applications, volume, p. 49 – 55 ,January 2007.
- [4] D., Gambetta and A., Ahfock, "New Sensorless commutation technique for brushless DC motors", IET Electric Power Applications volume 3, issue 1, p. 40 – 49, January 2009.
- [5] Jung-Hwan Kim, Sun-Kyu Kim, Joonhong Lim, "Commutation point estimation for Sensorless brushless DC motor using back-electromagnetic force change rate by least-square method", Electronics Letters, volume 51, issue 1, p. 31 – 33, January 2015.
- [6] Hussein Saberi, Mehran Sabahi, and Mohammad Bagher, "Improved Sensorless direct torque control method using adaptive flux observer", IET Power Electronics, volume 7, issue 7, p. 1675 – 1684, 2014.
- [7] H.C., Chen, C.M., Liaw, "Sensorless control via intelligent commutation tuning for brushless DC motor", IET Proceedings - Electric Power Applications, volume 146, issue 6, p. 678 – 684, 1999.
- [8] A., Ahfock, D., Gambetta, "Sensorless commutation of printed circuit brushless direct current motors", IET Electric Power Applications, volume 4, issue 6, p. 397 – 406, 2010.
- [9] Shao-Kai Tseng, Tian-Hua Liu, Jui-Ling Chen, "Implementation of a Sensorless interior permanent magnet synchronous drive based on current deviations of pulse-width modulation switching", IET Electric Power Applications, volume 9, issue 2, pp. 95 – 106, February 2015.
- [10] Wen-Chun Chi, Ming-Yang Cheng, and Cheng-Hu Chen, "Position-Sensorless method for electric braking commutation of brushless DC machines", IET Electric Power Applications, volume 7, issue 9, p. 701 – 713, 2013.
- [11] H.-B., Wang and H.-P., Liu, "A novel Sensorless control method for brushless DC motor", IET Electric Power Applications, volume 3, issue 3, p. no.240 – 246, May 2009.
- [12] H.C., Chen, Y.C., Chang, C.K., Huang, "Practical Sensorless control for inverter-fed BDCM compressors", IET Electric Power Applications, volume 1, issue 1, p. 127 – 132, January 2007.
- [13] E., Kaliappan, C., Chellamuthu, "A simple sensor-less control technique for PMSBLDC motor using back EMF zero crossing. European Journal of Scientific Research", vol.60 no.3, pp.347-360, 2011.
- [14] L., Topaloglu, F., Korkmaz, H., Mamur, R., Gurbuz, "Closed-Loop Speed Control of PM-BLDC Motor Fed by Six Step Inverter and Effects of Inertia Changes for Desktop CNC machine", Elektronika Ir Elektrotehnika, vol. 19, no. 1, pp.7-10, 2013.
- [15] Tae-Sung Kim, Byoung-Gun Park, Dong-Myung Lee, Ji-Su Ryu, and Dong-Seok Hyun, "A New Approach to Sensorless Control Method for Brushless DC Motors", International Journal of Control, Automation, and Systems, vol. 6, no. 4, pp. 477-487, August 2008.
- [16] C., Subba Rami Reddy & M., Surya Kalavathi, "Performance Analysis of BLDC Motor Drive using New Simulation Model with Fuzzy and ANFIS Speed Controllers", Global Journal of Researches in Engineering -Electrical and Electronics Engineering, Global Journals Inc. (USA), volume 14, issue 4 version 1.0, 2014.
- [17] Mehmet Cunkas, Omer Aydogdu, "Realization of fuzzy logic controlled brushless DC motor drives using MATLAB/SIMULINK", Mathematical and computational applications, vol. 15, no. 2, pp. 218-229, 2010.
- [18] Aamir Hashim Obeid Ahmed, Martino, O., Ajangnay, Shamboul, A., Mohamed, Matthew, W., Dunnigan, "A new technique for position control of induction motor using adaptive inverse control", Iraq Journal of Electrical and Electronic Engineering, vol.6 no.2, pp.116-122, 2010.
- [19] Jaijit Singh Changotra, Ramanand Harijan., "An adaptive filter as noise cancellation by using LMS/Newton algorithm" International journal on computer science and Engineering, vol. 4 No. 08, pp.1449-1453, 2012.
- [20] Matlab (R2008a), version 7.6.0.324
- [21] Hani Vahedi, Abdolreza Sheikholeslami, Mohammad Tavakoli Bina and Mahmood Vahedi, "Review and Simulation of Fixed and Adaptive Hysteresis Current Control Considering Switching Losses and High-Frequency Harmonics", Hindawi Publishing Corporation, Advances in Power Electronics, volume 2011, article id 397872, 6 pages, 2011.
- [22] V.M., Varatharaju and B. L., Mathur, "Adaptive Neuro-Fuzzy Speed Controller for Hysteresis Current Controlled PMSBLDC Motor Drive," 212 vol. 1, issue 4, pp. 212-223, 2011.
- [23] A., Purna Chandra Rao, Y., P., Obulesh, CH., Sai babu, "Performance improvement of BLDC motor with hysteresis current controller", International Journal of Advanced Research in Electrical, Electronics and Instrumentation Engineering, vol. 2, issue 12, pp.5900-5907, 2013.

IX. APPENDIX**3-PHASE INVERTER PARAMETERS**

Snubber Resistance-5000 ohms

Snubber Capacitance-1 μ F

Power Semiconductor Devices-IGBT and diodes

No of bridge arms-3

DC input supply voltage-300 V